PALACKÝ UNIVERSITY OLOMOUC

A DISSERTATION REPORT

Distance measurements with mode-filtered frequency comb and analysis of fluorescence from trapped ion at modulated dark state

Author:
Mgr. Adam LEŠUNDÁK

Supervisor:
Ing. Ondrej ČÍP Ph.D.

Department of Optics
&
Institute of Scientific Instruments of the CAS

Olomouc, May 6, 2019

Title:	Distance measurements with mode-filtered frequency comb and analysis of fluorescence from trapped ion at modulated dark state
Author:	Mgr. Adam Lešundák
Supervisor:	Ing. Ondřej Číp, Ph.D.
Ph.D. programme:	Optics and Optoelectronics
Institution:	Department of Optics, Faculty of Science, Palacký University
Year:	2019
External examiners:	

The thesis is available online at stag.upol.cz under Browse and Theses. The personal number is R120038.

This thesis is an original work of its author. All sources are cited under References.

PALACKÝ UNIVERSITY OLOMOUC

Abstract

Faculty of Science
&
Institute of Scientific Instruments of the CAS

This report presents the main methods and results of the thesis titled Distance Measurements with Mode-filtered Frequency Comb and Analysis of Fluorescence from Trapped Ion at Modulated Dark State.

The result of the first part of the thesis presents homodyne interferometry with a mode filtered frequency comb as a powerful method to measure long distances with high accuracy and absolute scale. The measurement principle requires that individual comb modes are spectrally resolved. For this reason the method cannot be applied directly to frequency combs with a low repetition rate (e.g. 100 MHz), since the modes are too close to each other to be resolved. Cavity mode filtering is used to increase the pulse repetition rate of a comb and the filtered comb is applied for mode-resolved absolute distance measurement. Mode-filtering takes place with a single Fabry-Pérot cavity in a Vernier configuration, allowing to set mode spacing ranging from tens of GHz to more than 100 GHz. It is demonstrated that large mode-spacing significantly reduce the requirements on the resolution of the spectrometer and enables absolute distance measurement with a mode-filtered frequency comb using a simple array spectrometer for detection. Here a 1 GHz comb is used, that is converted into a 56 GHz comb by mode-filtering. It is shown that in comparison to a conventional counting interferometer an agreement within 0.5 μm for distances up to 50 m is found.

The results of the second part of the thesis present a method using a single trapped $^{40}Ca^{+}$ ion as convertor from optical frequency domain to fluorescence intensity for optical frequency analysis of lasers interacting with the ion. The method is based on analysis of fluorescence emitted from the ion at a dark state excited by two laser fields with modulated mutual frequency detuning. The response of detected photon rate to relative laser frequency deviations is recorded within the slope of a dark resonance formed in the lambda-like energy level structure corresponding to two optical dipole transitions. Both employed lasers are phase locked to an optical frequency comb, which allows precise calibration of the method by deterministic modulation of the frequency modulated laser beam with respect to the beam with fixed optical frequency. Measured fluorescence responses are evaluated using the Fourier analysis and the results are compared with theoretical model for achievable signal-to-noise ratios in a range of modulation frequencies and amplitudes. The results shows the limits of this method in terms attainable modulation frequencies and detectable laser frequency deviations.

Acknowledgements

Many people stands behind the experiments presented in this thesis. Without their help and cooperation non of the results would be possible to achieve. My thanks goes to all of them and in special I thank my supervisor Ondřej Číp for giving my the opportunity to work on such extraordinary projects.

Also many thanks goes to Lukáš Slodička who was the main driving force and source of knowledge in the realization of the ion experimental setup and to Minh Tuan Pham, Peter Obšil and Martin Čížek for their scrupulous and consistent work on the preparation of the vacuum apparatus, ion trap and all the electronics.

Furthermore, I thank Steven van den Berg who has given me the chance to do my research at VSL and also Sjoerd van Eldik and Dirk Voigt for their endeavor on setting up the distance measurement interferometer and the spectrometers.

Finally, I am very grateful for generous support of my charming fiancée Petra Pokorná. I thank Petra for her encouragement, patience, strength and genuine love.

Contents

Chapter 1

Introduction

Light in the form of laser fields is used as indispensable tool in wide range of applications. Two of the fundamental metrology fields: distance measurements and optical frequency measurements are presented in the thesis. They both uses the optical frequency comb – form of light consisting of many coherent and tied waves within one optical beam. However, both applications are distinct in their nature and in the field of use, they both profit from the unique properties of the frequency comb laser. An optical frequency comb (OFC) is the spectrum of a laser whose optical modes are phase locked in such way, that they interfere together to form a train of pulses with a repetition rate frequency f_{rep} which directly represents spacing between neighboring modes in the frequency domain [1]. The nth comb mode frequency $f_n = \omega_n/2\pi$ is given by

$$f_n = n f_{rep} + f_0 \tag{1.1}$$

where f_0 is carrier-envelope offset frequency. Its development in 1999 [2, 3] caused a revolution in optical metrology. Frequency chains [4] previously used for absolute frequency measurements has been rapidly replaced by much simpler systems based on self-referenced frequency combs capable of covering large spectral ranges of hundreds of terahertz [5]. They provide direct traceability to a stable frequency reference such as a maser or an atomic clock [6]. In the past decades a wide variety of frequency comb applications has emerged, ranging from ultra-fast physics [7, 8], precise spectroscopy [9, 10] and astronomy [11, 12] to length metrology [13, 14].

There are two common types of optical frequency comb lasers distinct by the type of a laser gain medium and a passive mode locking mechanism. As representative of the first type, the early developed combs were based on titanium doped sapphire crystal (Ti:Sa) in a free space laser cavity. Later on a more robust and much less fragile second type – fiber frequency combs were introduced, where the gain medium is an optical fiber doped with Ytterbium or Erbium [15, 16]. Comb mode spacings are typically from tens to 250 MHz for fiber combs and roughly 80 MHz to 1 GHz for Ti:Sapphire combs. For distance measurements presented in this thesis a Ti:Sapphire comb with $f_{rep} = 1\ GHz$ and emission spectrum in region 810–830 nm is used. In measurements with trapped ions an Erbium doped fiber laser with $f_{rep} = 250\ MHz$ and emmision spectrum around 1560 nm, however frequency doubled and broadened to bandwidth ranging from 600 to 900 nm, has found its application .

Distance measurements with mode-filtered comb

In the first part of the thesis the optical frequency comb serves as a light source for optical distance measurements, while its properties are enhanced by a mode filtering optical cavity. This research have been carried out at Netherlands national metrology institute VSL in Delft as a part of the European Metrology Research Programme (EMRP) project “Metrology for long distance surveying”.

In the field of optical distance measurements a frequency comb can serve as a frequency reference to a continuous wave (CW) laser, which is then used as a light source for a displacement measurement. Other indirect methods for absolute distance measurement use the optical beat of two

CW lasers, whose phase shift of the synthetic wavelength determines the distance [17, 18]. Many schemes have been developed using the frequency comb itself as a light source for length metrology. One pioneering method was based on the heterodyne beat between longitudinal modes of a mode-locked laser [13]. An approach based on a time of flight of femtosecond pulses was later proposed [14], followed by several experimental demonstrations of cross-correlation based measurements [19, 20, 21, 22]. Homodyne and heterodyne interferometric schemes utilizing one frequency comb [23, 24] and two frequency combs [25, 26], respectively, have also been demonstrated. In 2012, Van den Berg established absolute distance measurements with a frequency comb laser, based on homodyne mode-resolved many-wavelength interferometry [24, 27]. The laser illuminates a Michelson interferometer, whose output is then spectrally resolved with a virtually imaged phased array (VIPA) spectrometer. The method allows for accurate measurements with a single frequency comb and a wide range of distance non-ambiguity. However it cannot be directly used with fiber frequency combs, which are better suited for potential field applications because of their ease of operation, robustness and smaller sensitivity to environmental disturbances. The reason for this is their small mode spacing of a few 100 Mhz, which cannot be resolved even with a VIPA spectrometer.

To enable the application of the method for low repetition rate frequency combs and also to enable the use of a simple grating-based spectrometer for detection, cavity mode filtering can be applied to increase the repetition rate of the laser source. The first implementation of external Fabry-Pérot cavity to a frequency comb was used for cavity-enhanced spectroscopy [9]. However, cavity filtering of frequency comb modes found its application soon after in astro-combs for calibration of high-resolution astronomical spectrographs [28, 11, 29]. Experimental work published on this topic describes in details the cavity filtering model with an effect of cavity-comb offset [30], selection of optimal cavity mirrors radius of curvature [31] or cavity dispersion [32].

A cavity mode filtering method, which uses the Vernier effect to enhance its performance, is presented. The mode filtered comb is then used for 50 m long distance measurements in laboratory conditions and the results are compared with a commercial fringe counting interferometer. Development of an all fiber approach for frequency comb mode filtering is also presented.

Fluorescence analysis

The second part of this thesis describes measurements carried out at my home Institute of Scientific Instruments of the CAS in Brno. Here a frequency comb is employed as a single optical reference for another lasers utilizing its stable frequency properties. The lasers are then used for interaction with a single calcium ion trapped in a Paul trap. The goal of presented measurements is to characterize ion fluorescence response to laser frequency deviations of two lasers driving appropriate atomic transitions. The ion serves as a convertor of optical frequency detuning of two interrogating lasers to photon fluorescence intensity. This approach is explored as a method of optical frequency analysis of optical fields separated by hundreds of THz, however within limited spectral range. The sensitivity of the fluorescence to relative frequency detuning of interrogating lasers is enhanced in the vicinity of a dark resonance.

Atoms with lambda-like energy level system are ideal for observations of this phenomenon. In such system destructive interference of amplitudes between two excitation paths from two ground states to an excited state leads to atom fluorescence quenching. Fluorescence spectrum of the atom close to the two-photon resonance is manifested with high photon count rate dependence on the mutual frequency detuning of the two excitation laser fields. These features called dark resonances have been found useful in many applications since their discovery by Alzetta et al. [33]. Various schemes of their use in laser cooling can be found [34, 35, 36, 37]. They can serve as a probe for motional state of single ion [38], or as a thermometer for trapped ions or ultracold atom cloud [39, 40].

To reveal possible applications and limits of the effect of optical two-photon interference with single atom as a tool for frequency metrology, we implemented a continuous measurement scheme on a single Doppler cooled calcium ion $^{40}Ca^{+}$ excited by two lasers at wavelengths 397 nm and 866 nm. The lasers are phase locked to common optical reference – the fiber frequency comb. Properties of the presented scheme are analyzed in terms of the fluorescence response to imposed laser frequency characteristics and measurement time. For this purpose, one of the lasers is frequency modulated, while the other has fixed frequency. Measured fluorescence responses are evaluated using the Fourier analysis and the results are compared with theoretical model for achievable signal-to-noise ratios (SNR) in a range of modulation frequencies and amplitudes. Finally we estimate the limits of the presented method and discuss comparison of measured data with simulations.

Chapter 2

Spectral interferometry

The principle of distance measurements presented in this thesis is based on spectral interferometry, which is a parallel homodyne interferometry with many spectrally resolved wavelengths [41]. A frequency comb with a multiplied repetition rate mf_{rep} is used as a light source. The distance is obtained from frequency dependent phase change of an interference signal, recorded by a spectrometer, that has distance-unique shape in the non-ambiguity range.

$$I(f) = 2\left|E_0\right|^2 \left[1 + \cos\left(\frac{2\pi \cdot 2L \cdot n_r \cdot f}{c}\right)\right]. \tag{2.1}$$

To employ the advantage of many optical frequencies in acquiring the distance, the phase change as function of frequency is utilized

$$\frac{d\Phi}{df} = \frac{4\pi L}{c}\left[n_r + f\frac{dn_r}{df}\right] = \frac{4\pi L}{c}n_g. \tag{2.2}$$

The distance L can be thus expressed as

$$L = \frac{d\Phi}{df}\frac{c}{4\pi n_g}. \tag{2.3}$$

In practice, the information about the phase change with frequency $d\Phi/df$ is obtained from the measured spectrum $I(f)$ by a cosine fit with $\Phi = C \cdot p + C_2$. In this equation C and C_2 are fitting parameters and p is a comb mode label associated to comb mode frequency $f_p = mf_{rep}(Q + p) + f_0$, where Q is a large integer number. Since the frequency comb is a periodic pulse train, the distance L is defined in a range of non-ambiguity $-\frac{1}{2}L_{pp} < L < \frac{1}{2}L_{pp}$, where pulse-to-pulse distance is

$$\frac{L_{pp}}{2} = \frac{c}{mf_{rep}n_g}. \tag{2.4}$$

Then a random distance is given by

$$L_t = \frac{1}{2}jL_{pp} + L. \tag{2.5}$$

Chapter 3

Frequency comb mode filtering

Cavity comb interaction

To describe the behavior of a frequency comb in an external cavity, firstly, we suppose that the cavity length is arranged to match the length of the laser cavity or that $FSR = f_{rep}$. This would ideally leads to the transmission of all comb modes.

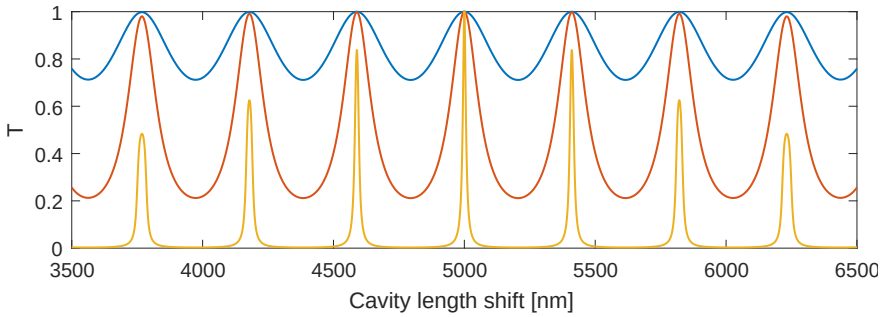

FIGURE 3.1: The cavity transmission of the frequency comb with central wavelength λ=820 nm, $f_{rep} = 1$ GHz and $f_0 = 0$ GHz as a function of the cavity length shift around length corresponding to FSR=1 GHz for 3 values of finesse F= 1, 3, 30 (blue, red, yellow).

With premise that the cavity dispersion is negligible and the comb is coupled to the TEM_{00} cavity mode, we compute the cavity transmission of the frequency comb as a function of cavity length L around value $L = \frac{c}{2FSR}$ for which

$$FSR = f_{rep}. \tag{3.1}$$

This corresponds to searching for a correct cavity length when parameters of the frequency comb are fixed. At this positions all comb modes are in resonance with cavity modes. The computation is done individually for each comb mode and then the sum of 10^4 modes is plotted in Fig. 3.1. The cavity transmission occurs at cavity length

$$L_c = \frac{c}{2f_{rep}}. \tag{3.2}$$

Since the cavity finesse is finite, non-exact solutions of Eq. (3.1) can be found. These solutions will result in a set of lateral transmission peaks. At this point $FSR \neq f_{rep}$, but nonzero linewidth $\Delta\nu$ of cavity modes allows for transmission of many comb modes. The cavity length can be unintentionally tuned into one of the lateral transmissions because their corresponding cavity lengths differ from L_c only in a nanometer range.

$$\Delta L_c = \frac{c}{2\nu}\frac{f_{rep}}{FSR} = \frac{\lambda}{2}. \tag{3.3}$$

Nonzero offset frequency f_0 will shift all transmission peaks, the central will become the lateral, eventually with an identical twin for $f_0 = f_{rep}/2$. The peaks height follows a transmission envelope shape.

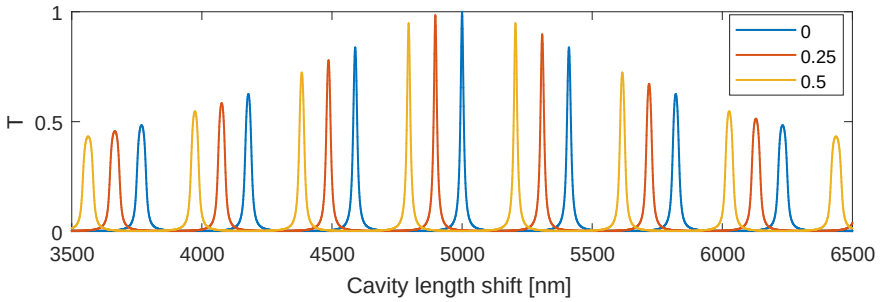

FIGURE 3.2: The cavity transmission as a function of length L for 3 values of f_0= (0, 0.25, 0.5)$\cdot f_{rep}$.

Since Eq. 3.2 holds only if the offset frequency f_0 equals zero, any offset frequency has to be compensated by slightly detuning the cavity by changing the cavity length by

$$\Delta L_{f_0} \approx \frac{\lambda}{2}\frac{f_0}{FSR}. \tag{3.4}$$

An example of the cavity transmission as a function of the cavity length and the effect of the offset frequency is shown in figure 3.2.

Frequency comb mode filtering

Frequency comb mode spacing, comfortably resolvable by a diffraction grating spectrometer is above 30 GHz. Such values can be achieved by setting the cavity FSR to an integer multiple m of f_{rep}, $FSR = m \cdot f_{rep}$. Such cavity arrangement is technologically very challenging, since it leads to cavity length $L_c \approx 0.5$ mm.

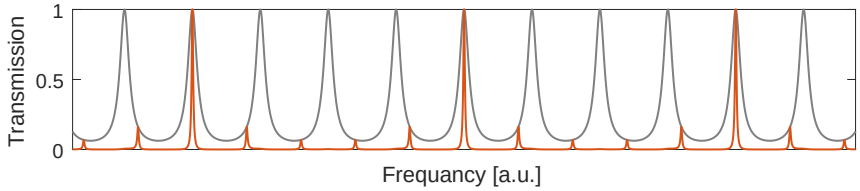

FIGURE 3.3: Example of low finesse $F = 6$ Fabry-Pérot cavity transmission (gray) with 1 GHz spaced FC modes (red). The cavity is set to Vernier configuration $4 \cdot FSR = 5 \cdot f_{rep}$. The FSR = 1.25 GHz, however 5 GHz spaced comb modes are transmitted.

A better solution to achieve such filter ratios has been found. The filtering method is based on the Vernier effect, with the cavity FSR set to a non-integer multiply of the f_{rep}

$$iFSR = mf_{rep}, \tag{3.5}$$

where i and m are integers. This is a scheme that is similar to frequency comb Vernier spectroscopy, see e.g. [12]. As a result we obtain a spectrum consisting of modes spaced by the lowest common multiple of the FSR and f_{rep}. Rewriting equation 3.2 in the Vernier configuration, the

cavity transmission occurs at cavity length

$$L_c = \frac{i}{m}\frac{c}{2f_{rep}}. \tag{3.6}$$

An example of the cavity transmission as a function of frequency is shown in Fig. 3.3. The advantage of the Vernier method is that the filter ratio is not inversely proportional to the cavity length and high filter ratios m can be obtained, via high values of the factor i, with a large mirror to mirror distance. This allows to build such a cavity with common optomechanical components and also to adjust the filter ratio ranging from 10 to infinity with small change of the cavity length. In practice, the largest filter ratio sufficiently filtering unwanted modes is proportional to the cavity finesse. For the distance measurements presented in this thesis, we used filter ratio of $m = 56$ and factor $i = 3$ corresponding to $FSR = 18.\bar{6}f_{rep}$. A simulation of the comb mode suppression for such parameters is in Fig. 3.4. The slight detuning of the cavity to account for nonzero f_0 leads to a small mismatch between the cavity resonance and the comb wavelengths. However, for an optical bandwidth of 14 nm, which is the spectral width of the Ti:Sapphire laser used in this thesis, it only leads to a 0.1 dB decrease of the transmitted signal in the wings of the spectrum.

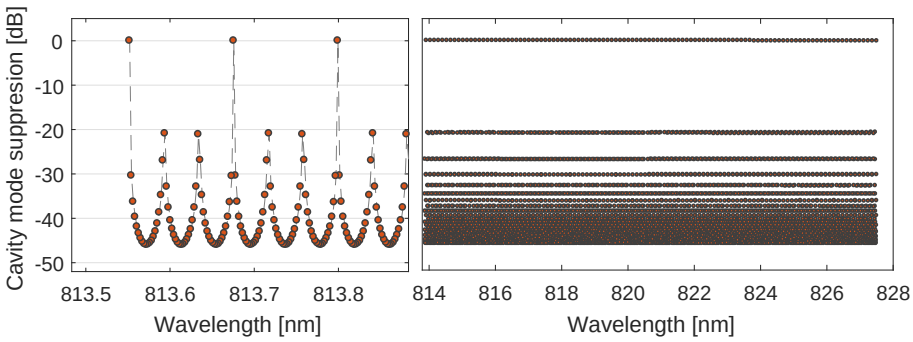

FIGURE 3.4: Simulation of frequency comb mode suppression by filter cavity with $FSR = 18.\bar{6}$ GHz. The comb repetition rate is $f_{rep} = 1$ GHz, the offset frequency $f_0 = 180$ MHz and the bandwidth of 14 nm is centered at 820 nm. With a cavity finesse $F = 313$ (mirror reflection 99%), the suppression of unwanted modes remains below -20 dB. The transmission of wanted modes is suppressed at the edges of the spectrum due to the offset frequency only by 0.1 dB. On the left side a small zoomed part of the spectrum is shown, to visualize individual modes. On the right side the mode suppression is shown for the full spectrum.

Chapter 4

Experimental setup for distance measurements

The experimental setup for the distance measurements can be divided into three main parts: a light source, a Michelson interferometer and a grating spectrometer, see Fig. 4.1. The light source is a Ti:Sapphire pulsed laser with the pulse repetition rate $f_{rep} = 1.012$ GHz and the offset frequency $f_{ceo} = 180$ MHz. The emitted optical spectrum is an optical frequency comb centered at wavelength $\lambda_c \approx 820$ nm with bandwidth of 14 nm.

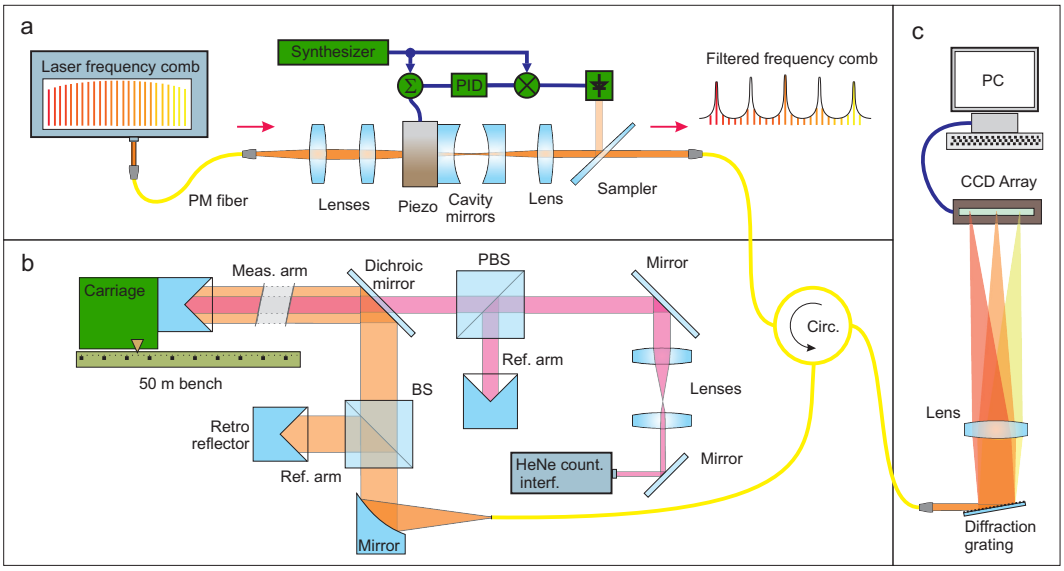

FIGURE 4.1: Experimental setup of the relevant parts for the distance measurement split into 3 sections. *a*) Filtering part showing the frequency comb laser, cavity mode-matching optics, cavity with piezo actuator, collimation lens and beam sampler. The green parts are the detector and electronics for locking the cavity length. The filtered frequency comb is led through an optical circulator towards the 50 m bench part. *b*) This part shows two Michelson interferometers with a common measurement arm for the filtered frequency comb and the He-Ne laser. *c*) Spectral analysis of the interferometer output with a diffraction grating and linear CCD camera.

The filter cavity based on two dielectric mirrors is used to increase the repetition rate of the frequency comb. The interferometer consist of two combined Michelson interferometers with common measurement arm, one is dedicated to frequency comb measurements and the other serves for comparison measurements utilizing a He-Ne continuous wave laser and interference fringe counting method. The spectral analysis is done with the grating spectrometer, however the VIPA spectrometer is also implemented into the setup for investigation of the filter cavity performance.

Filter cavity setup

The filter cavity setup consists of a Fabry-Perot cavity, cavity mode-matching optics and cavity-comb locking optics and electronics. A symmetric cavity was built with two concave dielectric mirrors with reflectivity of $R = 99.0\%$ and group delay dispersion below 20 fs^2. Each cavity mirror is attached to ring piezoelectric actuator for cavity length modulation and stabilization. For successful coupling of the frequency comb laser modes to the TEM_{00} mode of the optical cavity, a set of achromatic lenses are used to mode-match the laser beam to the cavity eigenmode and to collimate the cavity output.

Interferometer and spectrometer

The interferometer is located at the VSL long distance measurement laboratory. The laboratory is equipped with 50 m long rail bench. A commercial Helium-Neon laser fringe counting interferometer head (*Agilent*) is also part of the experimental setup and serves for the distance measurement comparison. The Michelson interferometer for frequency comb has common measurement arm with the counting interferometer.

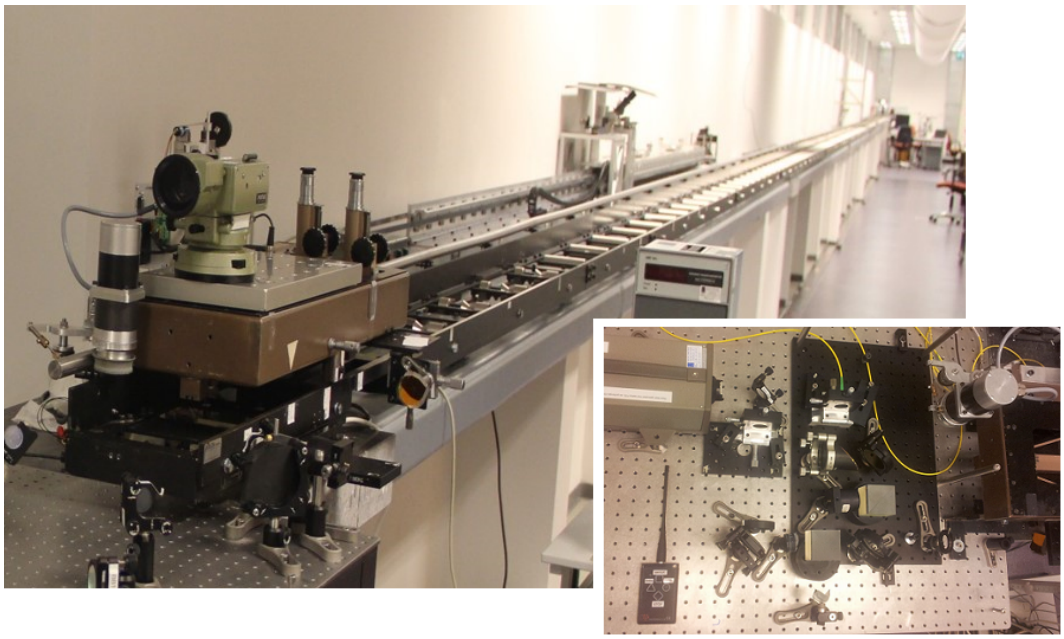

FIGURE 4.2: Large image: Long bench - the Michelson interferometer measurement arm with electronic carriage. Small image: interferometric head based on two inch sized optics.

The interferometer measurement arm has a maximum length of 50 m and consists of a long rail with electric carriage carrying the retroreflector, see Fig. 4.2. The comb beam is in the measurement arm mixed with the HeNe beam and as a result, both beams largely propagate through the same volume of air having the shared optical path. The reference arms for the comb and the HeNe laser are different, since the HeNe laser interferometer is based on measurements requiring a polarizing beam splitter. After propagation through the Michelson interferometer, a fiber circulator directs the FC interferometric output towards the spectrometers. The VIPA interferometer is implemented in the setup for diagnostic purposes. Returning beam from the interferometer is directed by the circulator to either the grating spectrometer or the VIPA spectrometer. Both spectrometers are mounted on transportable breadboards and for the experiments the breadboards are on the frequency comb optical table together with the filter cavity setup, pictured on Fig. 4.3. The grating spectrometer uses the source fiber connector ferrule as an entrance slit with 5 μm

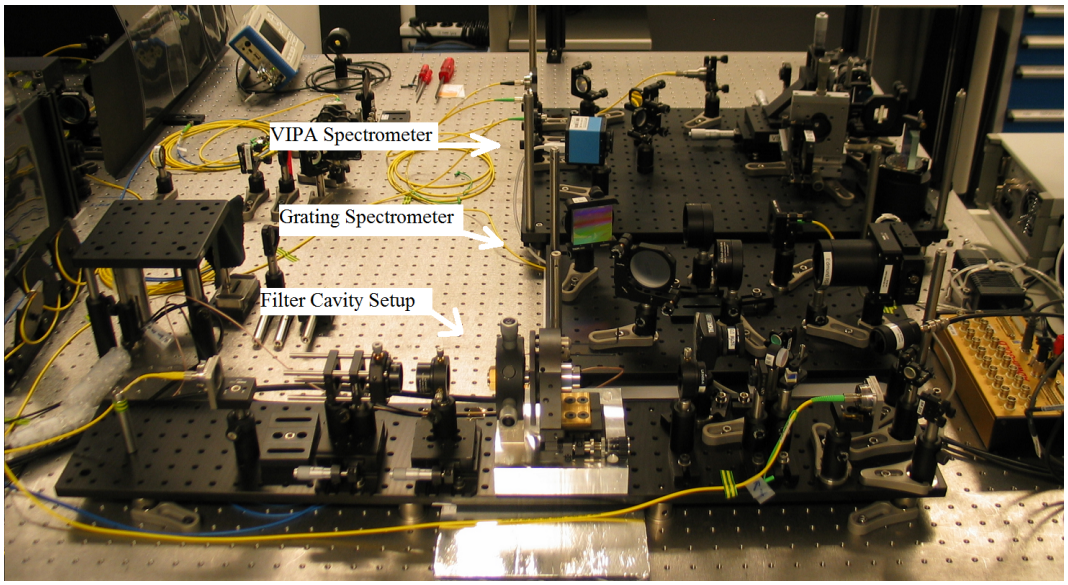

FIGURE 4.3: Three transportable breadboards, one with filter cavity setup and one for each of the spectrometers.

mode field diameter. The light is collimated by an achromatic lens with 100 mm focal length directly in grazing incidence onto a 50 mm wide reflective holographic diffraction grating with 1800 grooves/mm. The first order diffraction is focused with a 200 mm focal length achromatic lens on a sensor of CCD line camera. The camera has 3000 pixels, 7 μm pixel pitch and 200 μm pixel height. This configuration provides sufficient resolution to distinguish at least 20 GHz separated filtered comb modes, while capturing the full 20 nm wide spectral range of the comb spectrum.

The VIPA spectrometer is based on a VIPA etalon with 53 GHz free spectral range. VIPA etalon disperse the light in vertical direction towards a blazed diffraction grating with 1200 grooves/mm, which disperse the light in horizontal direction. A 400 mm focal length achromatic lens images the light on a CCD camera and creates 2D VIPA pattern.

Chapter 5

Measurements

This chapter describes the performance of the filter cavity by means of imaging the filtered frequency comb with the VIPA spectrometer and measurements of distances using the filtered frequency comb and the grating spectrometer.

Cavity filtration performance

When cavity length is scanned in the μm range its transmission shows many envelopes of transmission peaks. Each envelope corresponds different parameters i and m in the Vernier filtering condition $i \cdot FSR = m \cdot f_{rep}$. As an example, the second derivative of the cavity transmission is shown for cavity length scan with scanning range of about 1 μm showing the envelope for FSR = 20 GHz and approximately 100 μm scanning range around FSR ∼20.15 GHz with many envelopes.

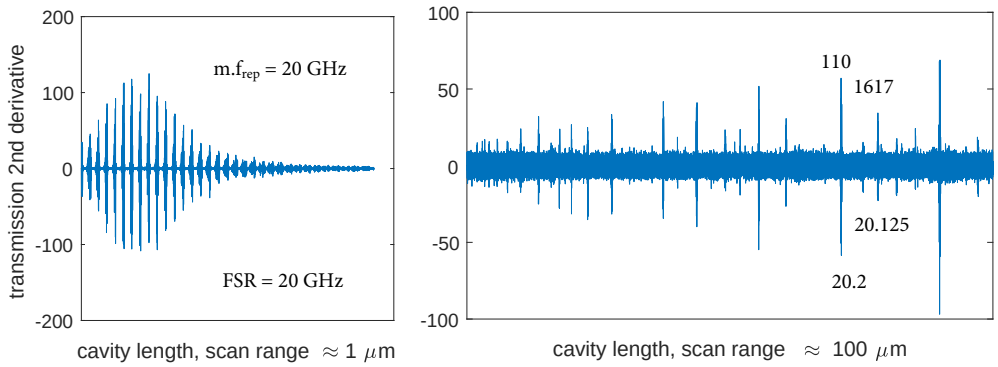

FIGURE 5.1: The second derivative of the cavity transmission as a function of cavity length. The transmission envelope for FSR=20 GHz – left, many envelopes within a 100 μm scanning range – right. The second derivative is used to enhance the visibility of the envelopes. Values of the cavity FSR and corresponding multiplied repetition rate $m \cdot f_{rep}$ are shown below respectively above envelopes.

Each envelope consists of a series of transmission peaks, as described in the chapter **??**. Locking the cavity to one of the peaks, represents a stable frequency comb filtration with a filter ratio m. Changing the ratio m multiple times in the Vernier configuration can be done by a fractional change of the cavity length. As can be seen in Fig. 5.1 in the vicinity of FSR = 20 GHz, there are visible transmission envelopes for $m \cdot f_{rep}$ in the THz range. The cavity filtering performance is diagnosed with the high resolution VIPA spectrometer. It resolves all the modes of the Ti:Sapphire frequency comb laser, separated by $f_{rep} \approx 1.012$ GHz, and creates an 2D image of dotted VIPA pattern. Each dot is an individual comb mode. In the vertical direction, dot-to-dot distance represents the f_{rep}, in the horizontal direction dot-to-dot distance represents the VIPA etalon FSR of 53 GHz.

The performance of the comb mode filtering is shown in Fig. 5.2 for four settings of the cavity FSR described in Table 5.1, note that an approximation of f_{rep}=1 GHz is taken in the table.

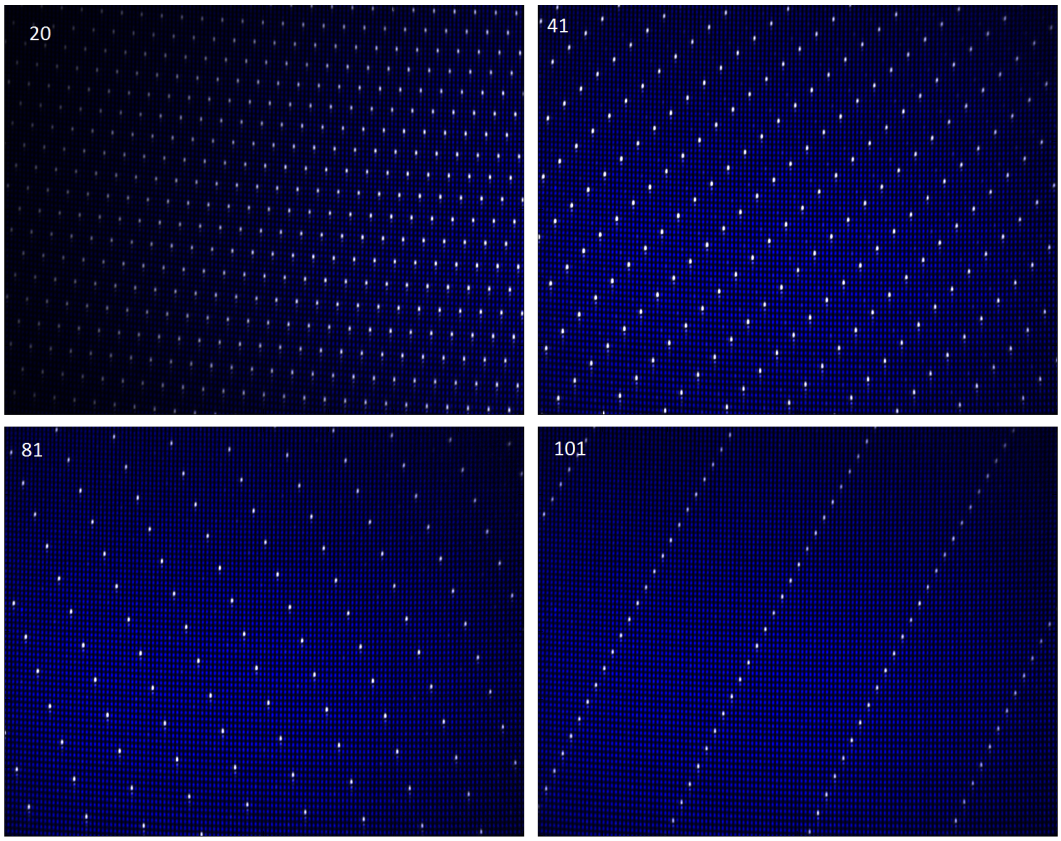

FIGURE 5.2: Composite VIPA spectra of the filtered frequency comb for four resulting values of $m \cdot f_{rep}$ = [20, 41, 81, 101] GHz (white dots) laying over the original unfiltered spectrum (blue dots)

L_{cavity} [mm]	7.50	7.43	7.41	7.32
FSR [GHz]	20	20.2	20.25	20.5
i	1	5	4	2
$m \cdot f_{rep}$ [GHz]	20	101	81	41

TABLE 5.1: Table of cavity settings fulfilling the vernier condition $i \cdot FSR = m \cdot f_{rep}$ for presented VIPA spectra.

Distance measurements

In this section a procedure and results of distance measurements using spectral interferometry with mode filtered frequency comb and diffraction grating spectrometer are presented. The length of the filter cavity is set at 8.0 mm, corresponding to a $FSR = 18.\bar{6} f_{rep}$, which due to Vernier selection, results in a filter ratio $m = 56$. This corresponds to a pulse-to-pulse distance $L_{pp} = 5.3$ mm. The distance measurements are performed quasi-simultaneously with the Helium-Neon laser fringe counting method, which serves as comparison. The results are then presented as a difference between the two methods [41]. The reference data from the measurement I_{meas} and reference I_{ref} arms are used for intensity normalization of interference spectrum I as shown in Fig. 5.3

$$\cos(\Phi) = \frac{I - I_{ref} - I_{meas}}{2\sqrt{I_{meas} I_{ref}}}. \tag{5.1}$$

From its cosine fit the distance L is calculated. The results in Fig. 5.4 show the differences between the individual measurements done by frequency comb and the average distance as measured with

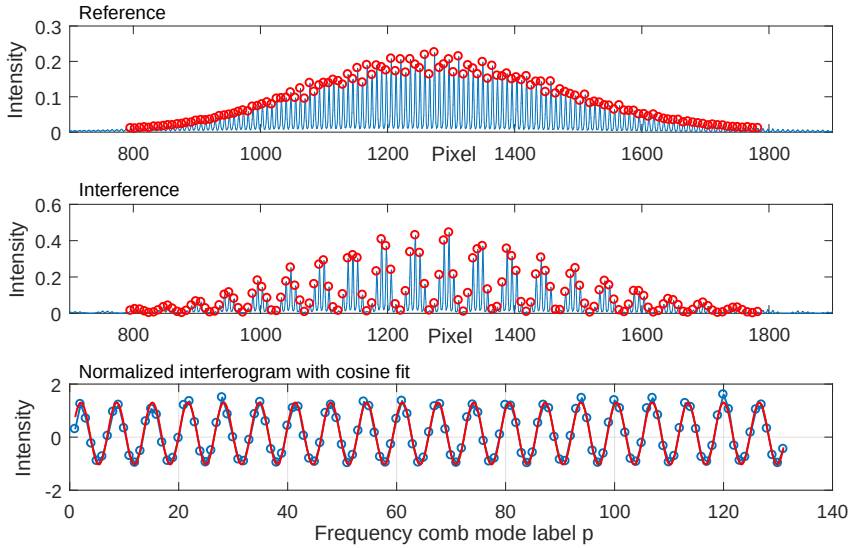

FIGURE 5.3: Top: typical reference measurement-blue, I_{ref} intensities - red circles. It is used for correct finding of the comb mode positions at CCD and also for the interference normalisation. Middle: interference measurement - blue, with values of $I(f)$ intensities - red circles. Bottom: normalized intensities $I(f)$ - blue circles and cosine fit - red.

the HeNe counting interferometer. The zero position is based on the average of the five zero measurements. For each individual measurement the agreement between the frequency comb and the HeNe laser is within 0.8 μm. When averaged over five measurements, the largest difference is 250 nm. The standard deviation doesn't show a clear distance dependence and is on average 0.33 μm. The comparison measurement shows that the mode-filtered frequency comb is a suitable tool for distance measurements, with a relative difference $< 10^{-8}$ with the HeNe laser reading for a distance of 50 m. The observed differences between both methods for a single measurement are caused by environmental effects, like turbulence and vibrations. These effects are not perfectly canceled because of small timing differences between the simultaneous HeNe and comb measurements. When averaging all measurements and all distances, the agreement between both methods even reduces to below 100 nm.

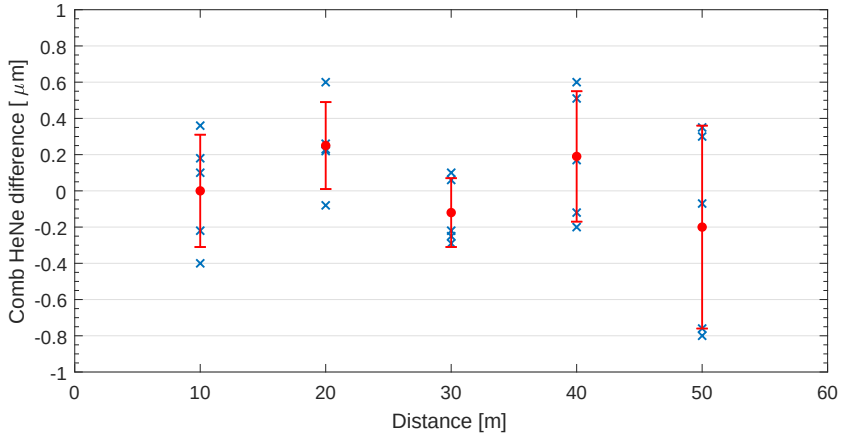

FIGURE 5.4: Measured differences between distance measurement with a filtered frequency comb and a HeNe laser interferometer for distances up to 50 m. The error bars show the standard deviation of the measurements.

Chapter 6

All fiber filter cavity approach

This chapter briefly describes an alternative method of frequency comb mode filtering based on a single mode optical fiber cavity. The aim for the development of such a tool is its simplified implementation into an optical setup. No requirement for any mode-matching optics allows for plug-n-play by simple connecting the fiber cavity to an input and output optical fibers. Different fiber based comb mode filtering has been published, with use of a fiber coupled free space cavity [42], ring fiber resonator [43] and cascade Mach-Zhender fiber interferometer [44] or more recently a few meter long single optical fiber [45].

Fiber cavity design

Principle construction of presented fiber cavity is the same as of a free space cavity. There are two reflecting surfaces at the ends of the fiber. Lateral cavity modes are tuned by fiber stretching. The maximal amount of reversible stretching is not precisely known but approx. 0.5% of the fiber length is considered as safe.

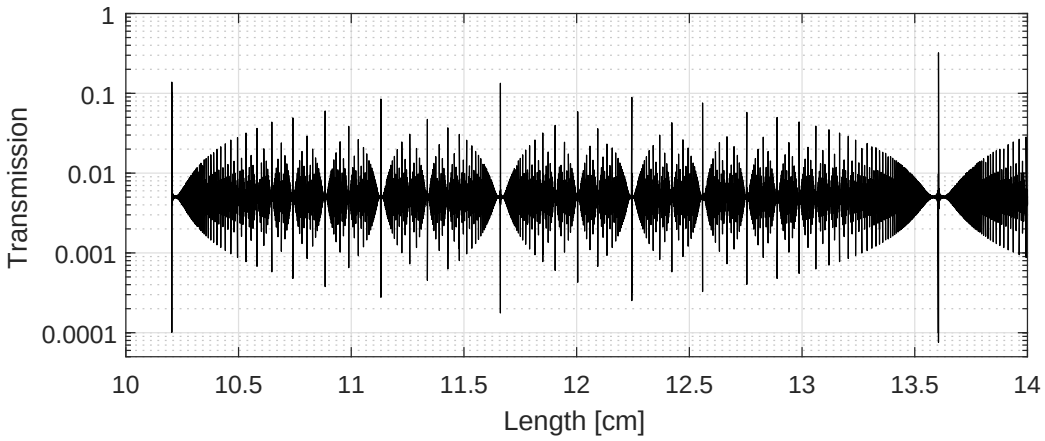

FIGURE 6.1: Silver-coated-fiber cavity transmission of a 100 MHz frequency comb as a function of length. Theoretically, infinite number of transmission envelopes is available.

Although a fiber cavity cannot be stretched in order of cm, Fig. 6.1 shows calculated cavity transmission of frequency comb modes for such range in order to highlight the amount and positions of Vernier transmission envelopes. The first generation of a fiber cavity is designed to work with an Er^3+ fibre based frequency comb with central wavelength at 1550 nm. Its free spectral range is designed to be FSR=1 GHz. Fiber with near zero dispersion is used for fiber patchcord production. The fiber length corresponding to FSR = 1 GHz is L_{fiber}=102.1 mm but actual length of fiber patchcords is designed to be 101.8 mm. The production has been carried out by *SQS Vláknová Optika a.s.*, where the fiber was cut to predefined length and equipped with FC/PC type ceramic ferrules and connectors. Cavity mirrors are created by sputtering of a reflective material directly on the fiber patchcord ends. A 40 nm thin layer of Ag has ∼95% reflectivity and ∼1.5%transmission, the rest of light ∼3.5% is absorbed. Reflective layers are created by magnetron

sputtering deposition at ISI Brno by the Thin Layers group. A cage mounting system is used for holding the fiber cavity and to adjust its length. Two standard fiber connectors are mounted to the cage, one with help of a custom made adapter, the other is attached to a manual translation mount via a custom made adapter with a ring piezochip. The fiber length can be stretched and electronically locked to a required transmission peak. The cavity length is stabilized with the same locking technique as the free space cavity, however using only one piezochip for both, modulation and stabilization.

Results

The cavity filter properties were tested at the TU Delft, The Department of Imaging Physics. The fiber frequency comb they possess has repetition rate f_{rep} = 100 MHz. The cavity multiply the original f_{rep} to $m \cdot f_{rep}$ = 1 GHz, in a normal configuration $i \cdot FSR = FSR$ (not Vernier, $i > 1$). The cavity comb mode filtering is observed with a TU Delft VIPA spectrometer. The VIPA spectrometer is not able to resolve modes of the fiber frequency comb. In the VIPA spectral image the modes merges into lines. However it is able to resolve less dense modes of the filtered frequency comb which are observable as dots, see figure 6.2. The presented result shows that an optical frequency

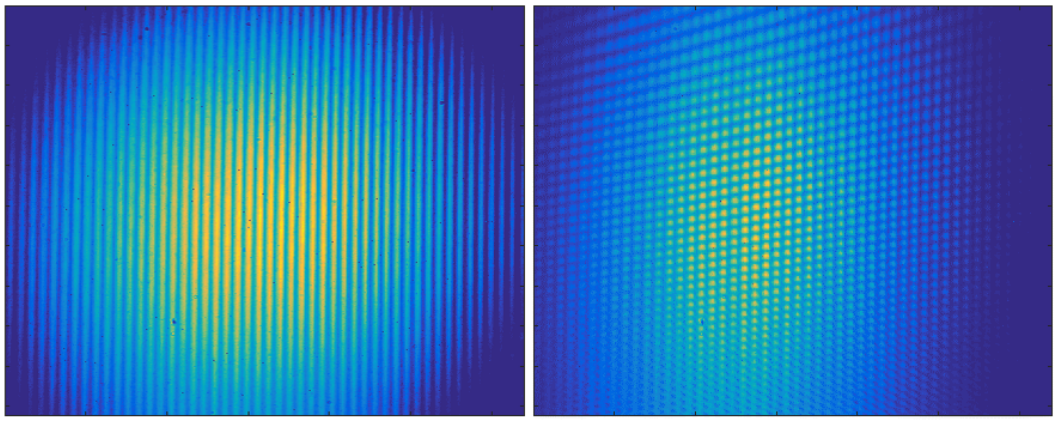

FIGURE 6.2: VIPA images for frequency comb with f_{rep} = 100 MHz - left and fiber cavity multiplied f_{rep} = 1 GHz - right.

comb can be filtered by a fiber based filter cavity. Further development of this method has been started. Fiber patchords in the Vernier configurations has been designed using dielectric layers with zero chromatic dispersion and reflectivity of more than 99% instead of the silver reflective coatings. However, this second generation of the fiber cavity has to be yet properly tested.

Chapter 7

Ion experimental setup

The aim of the experiment discussed in the second part of the thesis is to analyse the fluorescence response of a calcium ion stored in a radio frequency trap to modulation of frequency detuning of two excitation laser fields. We are particularly interested in the characterization of fluorescence sensitivity to laser frequency detunings mediated by the ion in a dark state. This measurement is explored as a method for optical frequency analysis using the ion as a convertor of the relative optical frequency difference to the intensity of emitted fluorescence from the ion. The main goal is to provide a characterization and point out limits of this method. The dark resonance not only enhances the spectral sensitivity but, it allows for optical frequency beating of two optical fields separated by hundreds of THz, which corresponds to a frequent task in many metrological applications [4, 5, 46]. This is typically realized indirectly via an optical frequency comb. The presented method provides an alternative to these methods within limited spectral range, however the frequency comb serves here as a stable optical reference for the excitation lasers.

The experimental setup for ion trapping is newly build in the laboratories of the Institute of Scientific Instruments of CAS in Brno. On its set up cooperated colleagues from the ISI Brno and from the Department of Optic of Palacký University Olomouc. On the development of the vacuum apparatus was also involved Mesing company and the Paul trap was designed and fabricated at the University of Innsbruck.

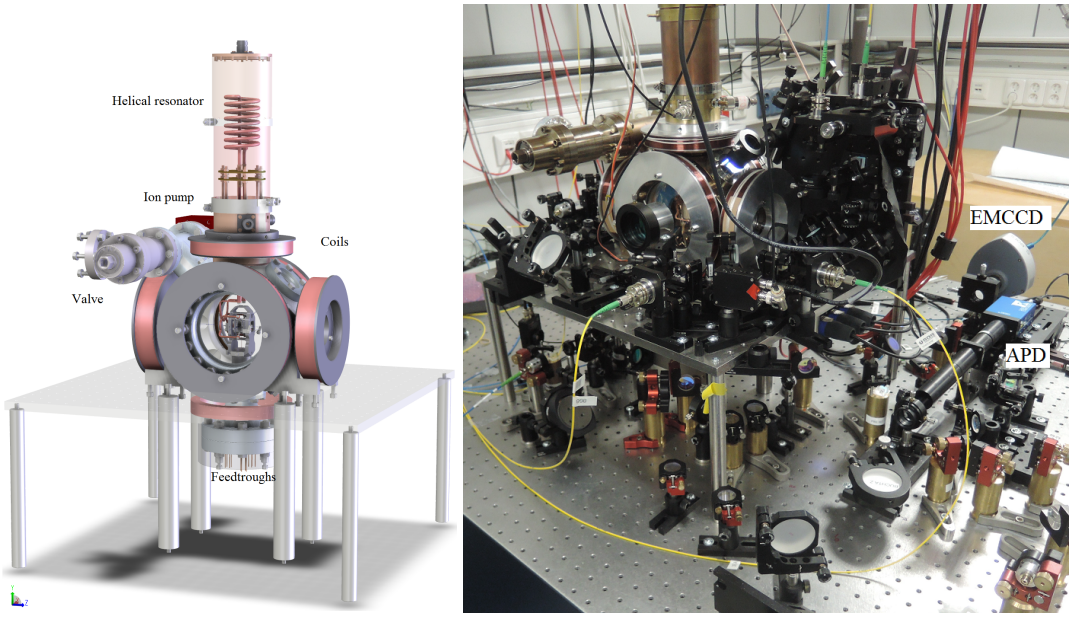

FIGURE 7.1: Scheme of the complete vacuum chamber setup with Paul trap inside – left. Actual picture of the vacuum chamber with optical components for ion interrogation – right.

Laser stabilization

The fluorescence analysis described in the thesis requires highly stable optical frequency per-

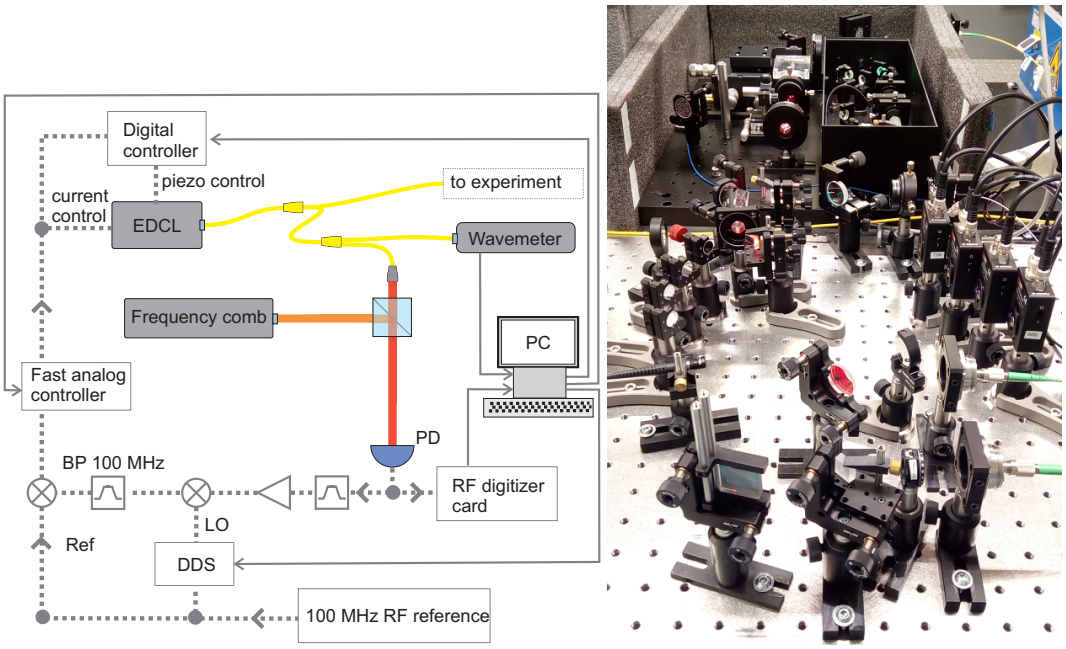

FIGURE 7.2: Schematic view of the phase locking of an ECDL to frequency comb, however for simplicity shown only for one laser – left. The real optical part of the scheme for five lasers is shown in the picture on the right. Top of the picture shows supercontinuum generation. At the bottom is diffraction grating separating mixed laser beams, which are then with mirrors on the left reflected to detectors on the right. (Only two used for the experiment.)

formance of the 397 nm and 866 nm lasers. For this reason both lasers are phase locked to a corresponding tooth of the optical frequency comb. A scheme of electronics and picture of optics for phase locking are in Fig. 7.2. The frequency comb with a center frequency at 1560 nm is frequency doubled by second harmonic generation (SHG) process in and then broadened by a photonic crystal fiber to generate an optical supercontinuum ranging from about 600 to 900 nm. This broad spectrum is mixed with laser beams to create beat notes with particular frequency comb tooth. The beat note signal is used as an input for phase locked loop (PLL), which efficiently narrows the laser linewidth down to linewidth of a single component of the frequency comb. Particular beat note signal between the comb tooth and the laser is amplified, filtered and mixed with a local oscillator (LO). This LO is generated by a direct digital synthesizer (DDS) referenced to the hydrogen maser, and has the value of the desired beat note frequency raised by 100 MHz. After bandpass filtering, the product of mixing is mixed once more with 100 MHz reference signal to generate a DC signal which has the phase information of the comb-laser beat note and serves as the error signal for laser phase-locked loop (PLL). The PLL is realized with fast analog control electronics. The target frequency of atomic transition is achieved by a fine frequency tuning with an AOM in double pass configuration. These AOMs are also used for amplitude stabilization of the laser intensities. An overview of the experimental setup is shown in Fig. 7.3. It is separated to the tree optical tables dedicated to the ion lasers, frequency comb and laser beating and the table with the ion trap.

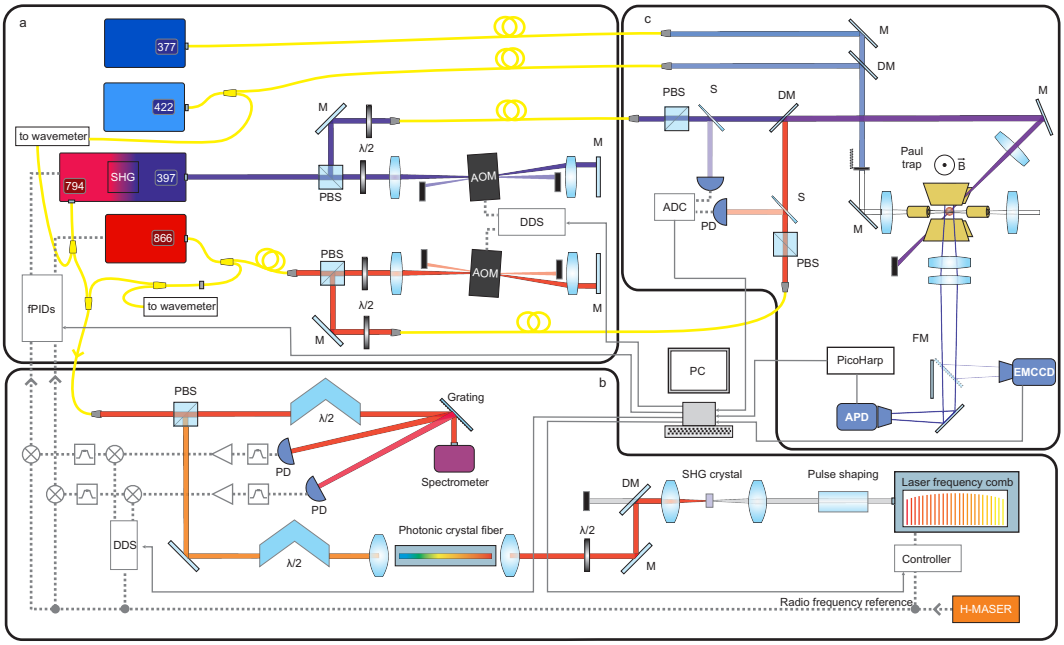

FIGURE 7.3: Scheme of the experimental setup distributed over three optical tables corresponding to parts a), b), c). All ion ECDLs are placed on table a). The cooling laser beam is generated by frequency doubling the 794 nm to 397 nm. The near infrared laser beams are send through an optical fiber to table b) where the optical frequency comb supercontinuum is optically mixed with lasers by use of broadband optical elements and the products are spatially separated for beat note detection. Individual beat notes are after filtering and amplification used for generating the control signals for frequency stabilization of the lasers. The 397 nm and 866 nm laser beams dedicated to the ion are led into AOMs in the double pass configuration for frequency and amplitude modulation and then sent to the ion trap positioned on the optical table c). The laser fields are set to particular desired polarization and are amplitude-monitored at the proximity of the ion chamber. The ionization laser are send directly to the ion only with 422 nm wavemeter-based control. A beam shutter blocks the ionization lasers after successful loading of desired number of ions. The ion fluorescence is collected by a lens with Numerical aperture of 0.2 and detected by the EMCCD camera or single photon avalanche photdiode. The detection signals including precise photon arrival times are recorded using fast time-tagging module or converted by an analog-digital card (ADC) for further processing.

Chapter 8

Analysis of fluorescence of ion at modulated dark state

A continuous measurement scheme on a $^{40}Ca^{+}$ ion with the transitions $4S_{1/2} \leftrightarrow 4P_{1/2}$ and $4P_{1/2} \leftrightarrow 3D_{3/2}$ excited by two lasers fields at wavelengths 397 nm and 866 nm is implemented. The 397 nm laser is also used for simultaneous Doppler cooling, while 866 nm repumps the ion from a long lived $3D_{3/2}$ manifold. Both lasers are phase locked to the fiber frequency comb, which allows for precise calibration of optical frequency analysis by deterministic modulation of the analyzed laser beam with respect to the reference beam. For this purpose, the repumping laser serves as an analyzed field to which a deterministic frequency modulation is applied, while the cooling laser is the reference field with fixed frequency. Properties of the presented scheme are analyzed in terms of the fluorescence response to imposed laser frequency characteristics [47].

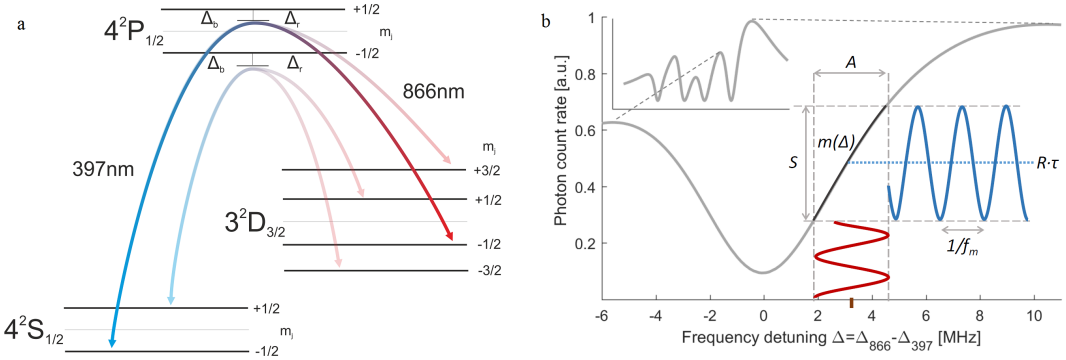

FIGURE 8.1: Scheme a) shows the employed energy level scheme of $^{40}Ca^{+}$. The two laser fields with polarizations perpendicular to the magnetic field lead to observation of four dark states between $S_{1/2}$ and $D_{3/2}$ manifolds. Scheme b) shows a simulation of the $P_{1/2}$ level occupation probability proportional to fluorescence intensity as a function of 866 nm laser frequency detuning Δ_{866}. Detailed zoom in the selected dark resonance depicts the fundamental parameters determining the performance of the spectral analysis including the detuning Δ_{866}, frequency deviation of the frequency modulation A, modulation frequency f_m, conversion through the slope with parameter m onto the fluorescence with average photon count rate per second R_s and measured with an APD gate time τ.

The trapped and Doppler cooled ion is simultaneously driven by two laser fields at 397 nm and 866 nm. Applied magnetic field lifts the degeneracy of the Zeeman states, which results in energy level scheme with eight states, see Fig. 8.1*a*. The angle between polarization of the laser fields is chosen to be perpendicular to the magnetic field, therefore only transitions with $\Delta m_j = \pm 1$ are excited, which leads to the observation of four dark resonances. Fluorescence from the ion is collected in the direction of the magnetic field using objective lens with numerical aperture of 0.2 and focused onto the free spaced APD. Time tags of photon detections are recorded with fast time

tagging module. Tuning the 866 nm laser to a position at a slope of particular dark resonance, described by a slope parameter $m(\Delta_{866})$ representing the resonance gradient, allows to use the ion as a direct frequency deviation to fluorescence intensity convertor due to its high and quasi-linear dependence, see Fig. 8.1*b* for schematic explanation.

Fluorescence spectra with phase locked lasers

Figure 8.2 illustrates the enhancement of the dark resonance contrast and slope steepness by

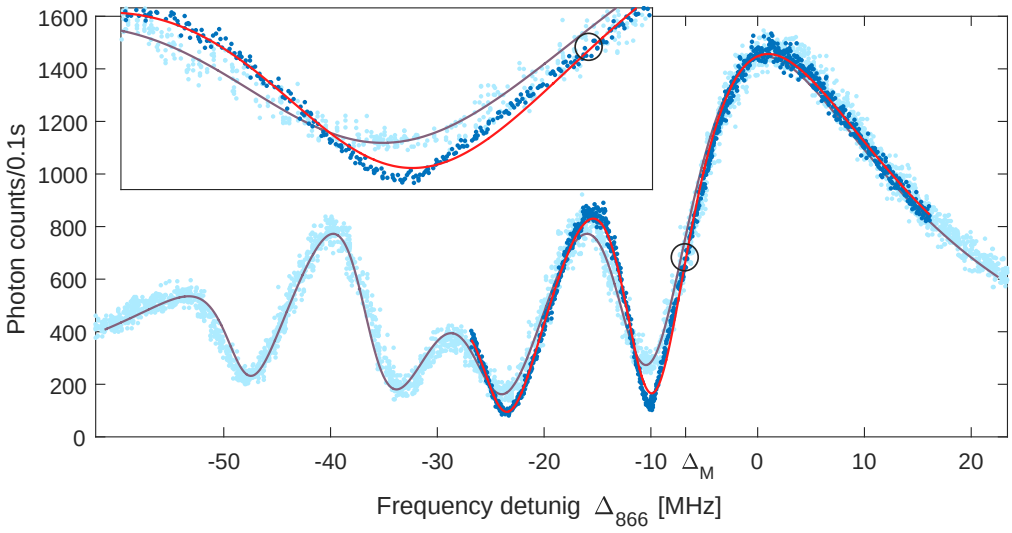

FIGURE 8.2: Dark blue fluorescence spectrum measured with both lasers phase-locked to the frequency comb with limited bandwidth due to PLL limited scanning range. Red line is the optical fit and black circle corresponds to the measurement point. Parameters of the fit are the magnetic field $\vec{B}$ = 6.1 Gauss, the detuning of the blue laser from the degenerate transition Δ_{397} = -16 MHz, angle between the light fields and the magnetic field α = 90°, saturation parameters S_{397} = 1, S_{866} = 4 and combined linewidth of the two lasers Γ =124 kHz.Light blue is fluorescence spectrum with all dark resonances visible, measured by scanning of free running 866 nm laser monitored by wavemeter. Purple line is its fit with the only parameter significantly different from the PPL scan being the lasers combined linewidth Γ = 250 kHz. The insertion shows the lower part of the resonance with the measurement point. Difference in the resonance depth for the two spectra is clearly visible. The shape of the PLL resonance also does not perfectly fit to the theory .

utilization of frequency stabilization of 397 nm and 866 nm lasers to the frequency comb. The fluorescence spectrum is measured , however in narrow bandwidth limited by the PLL frequency scanning range of f_{beat} from 0 to 125 MHz. The whole spectrum containing all dark resonances is measured again, but with 866 nm laser frequency controlled utilizing only the wavemeter-based feedback. Both fluorescence spectra are fitted with the optical Bloch equations.

Measurements of fluorescence response

The frequency spectrum of the analyzed 866 nm laser deviations is measured by keeping the reference 397 nm laser at constant detuning Δ_{397} and modulating the frequency detuning $\Delta_{866}(t)$. To determine the theoretical response function of the detected fluorescence to the introduced frequency modulation a natural fluorescence noise is compared to the observable signal in the evaluated frequency spectrum of the fluorescence. Equation for the fluorescence signal to noise ratio SNR is derived as the ratio of function describing the amplitude of harmonically modulated fluorescence $S(f_m, A, \tau)$ to the amplitude of fluorescence noise $N(R, T, \tau)$

$$SNR = \frac{S}{N} = \sqrt{\frac{T}{R\tau}} mA\tau \left|\mathrm{sinc}(f_m\tau)\right| . \tag{8.1}$$

The measurements of fluorescence response are done for various sets of modulation frequencies f_m, frequency deviations A, measurement time T and also measurement points Δ_M. A fluorescence time tag measurement is processed into set of fluorescence data in units of photon counts per τ, where τ has values from a certain range simulating a variable gate time of a photodetector. These data are then individually analyzed in terms of their frequency spectrum evaluated by the FFT algorithm. The values of signal-to-noise ratio are then $SNR = S_{meas}/N_{meas}$, where S_{meas} is the frequency component at the modulation frequency f_m (or component with maximal amplitude) and N_{meas} is the average amplitude of the whole FFT spectrum. The results of frequency response measurements are summarized in four figures. Three of them emphasize the $SNR(\tau)$ dependence on the critical measurement and evaluation parameters, in particular modulation frequency Fig. 8.3, frequency deviation Fig. 8.4, and measurement time 8.5 with respect to the gate time τ. The last figure compares the $SNR(\Delta_M)$ for two modulation frequencies with respect to the measurement point Δ_M which corresponds to different values of count rate R_s and slope parameter m Fig. 8.6.

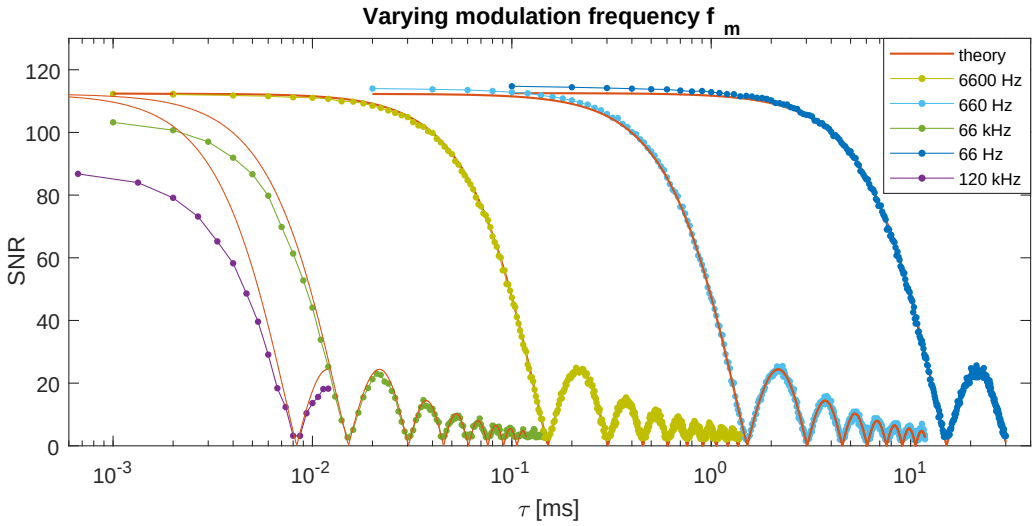

FIGURE 8.3: Signal to noise data for five 300 s long measurements of fluorescence with modulated detuning Δ866. Frequency deviation is kept at 300 kHz and modulation frequency varies - dots. Red lines - theoretical signal to noise ratio calculated using nonlinear slope function $m_n l$. Note that mean time between two successive photon detections is ~ 0.15 ms.

The lowest detectable signal in the frequency spectrum has its limit given by frequency amplitudes of shot noise. This detectable limit is defined here as variable SNR_{lim}. The limit is obtained by simulating data of shot noise with Poissonian distribution. The simulated data represents pure fluorescence without modulation and have the same count rate R and measurement length T as the real data.

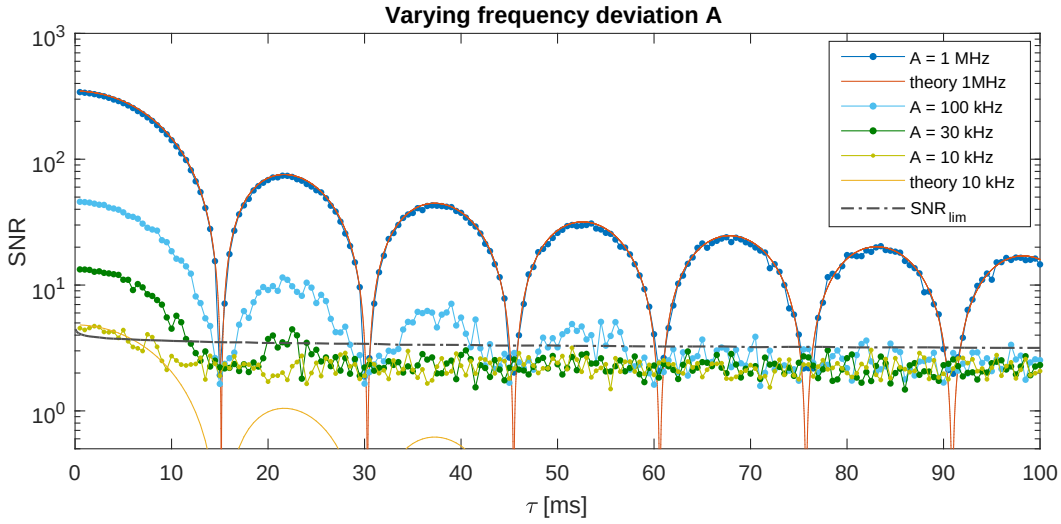

FIGURE 8.4: Signal to noise measurements of fluorescence with harmonically modulated detuning of analyzed laser field Δ_{866} with modulation frequency set to 66 Hz. The measured data for different frequency deviations are shown with dots with lines. Full lines show the theoretical simulation of SNR for the highest and lowest frequency deviations, respectively. Dash-dotted gray line represents a numerical limit given by pure signal with Poisson distribution evaluated as maximal amplitude of shot noise. Amplitude levels for signals are taken from known frequency position in the spectrum, thus the fringe pattern is slightly visible even below the limit.

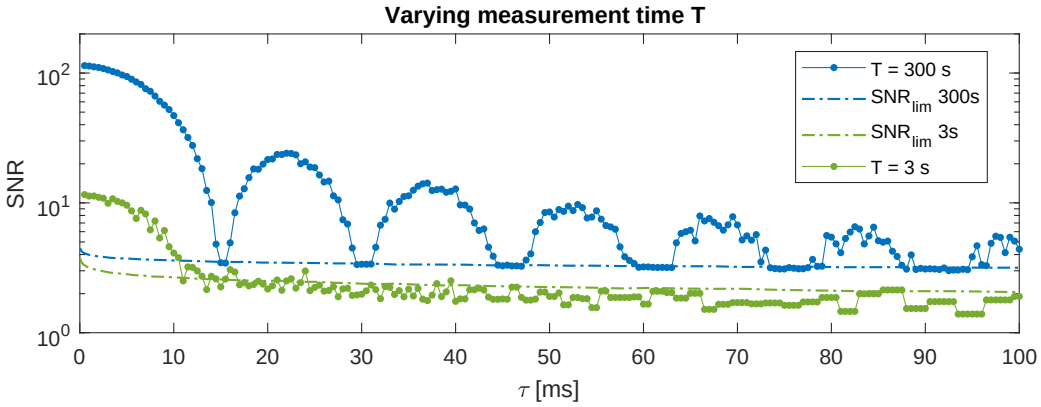

FIGURE 8.5: SNR data for 3 s and 300 s long measurement of fluorescence with harmonically modulated laser detuning Δ_{866}. Modulation frequency and frequency deviation are fixed to 66 Hz and 300 kHz, respectively. The signal amplitudes are found as the maximum of whole frequency spectrum except the DC component. The dots show the measured data, dashed lines represent numerical limits given by simulated fluorescence with Poisson distribution SNR_{lim}.

The results of presented measurements are interpreted in here in terms of fundamental limits of the proposed method. Fluorescence sensitivity to frequency deviation A is given by the slope function of the dark resonance m, which depends on the parameters of applied magnetic and laser fields. The measurement point used for the measurements with variables A, T and f_m is no worse (in terms of fluorescence gradient) than $1/2$ of the steepest slope of any dark resonance achievable by tuning the parameters of applied fields to the ion. It however stands on the slope, whose length in the axis of frequency detuning, has been set by the parameters to ~ 8 MHz. This gives a fundamental upper limit of the presented method on the optical frequency bandwidth which does

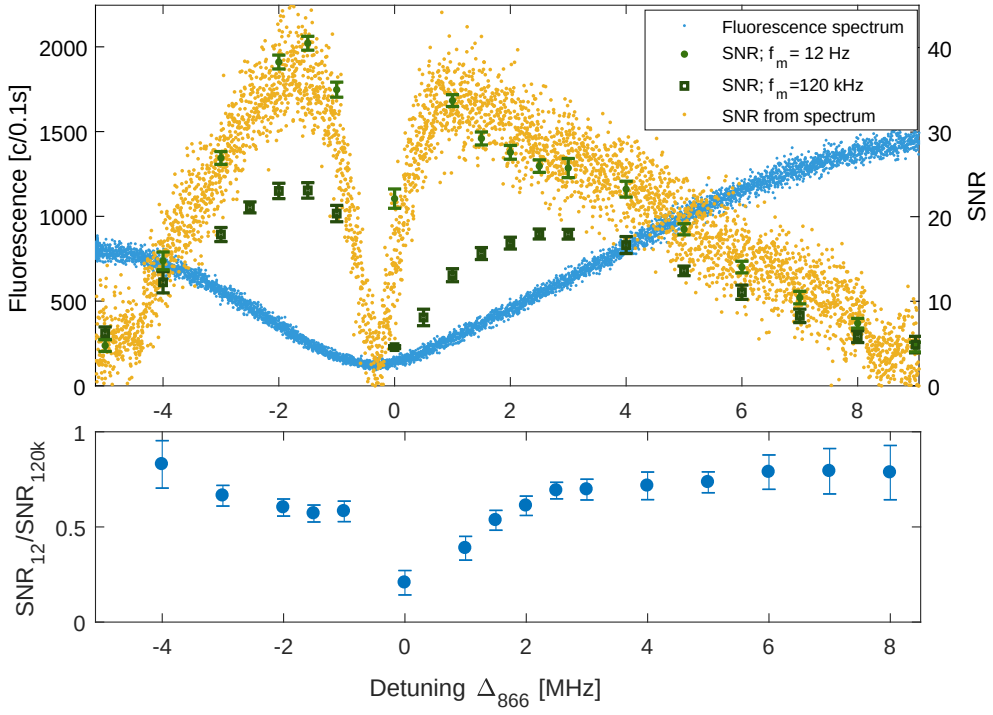

FIGURE 8.6: Upper graph shows theoretical data of SNR data – orange dots calculated on basis of measured fluorescence spectrum – blue dots. Average SNR of ten measurements with T = 10 for two modulation frequencies 12 Hz – green circle, 120 kHz – green square are measured along the dark resonance. Errorbars corresponds to two standard deviations. Ratio between measured SNR for the two f_m data sets is shown on the lower graph.

not cause 866 nm laser to detune out of the resonance slope. The width of the employed dark resonance slope and the measurement position on the slope thus limits the frequency deviation and modulation frequency. According to the Carson rule for frequency modulation bandwidth with 98% of modulation energy [48, 49], combined frequency deviation A and modulation frequency f_m has to satisfy condition $2(A + f_m)$ = 8MHz. This condition is well satisfied in the measurements. The smallest detectable modulation amplitudes are given by fluorescence noise at given photon count rate and total length of the measurement. This limit is defined as SNR_{lim} and corresponds to ratio of maximal amplitude in a pure shot noise frequency spectrum with its mean value N. Scale up in the measurement time T leads to raise of the SNR_{lim} limit value, however the mean level of amplitudes of shot noise frequency spectrum N is proportional to $\sqrt{R\tau/T}$, thus the lowest detectable frequency deviation can be scaled down with longer measurement times or by measuring in the lower part of the resonance slope with smaller photon count rates. Specifically for measurement at point Δ_M with the linear slope parameter m = 1.78 cps/kHz, count rate R_s = 6800 cps, measurement time T = 300 s, gate time τ = 1 ms and modulation frequency f_m = 66 Hz, the limit of detectable frequency deviation is A_min = 2 kHz.

Detectable modulation frequency is according to the presented theory in Eq. (**??**) unlimited, however, the presented measurements show decrease of $SNR(f_m, \tau)$ for high modulation frequencies. In our particular case, the decrease has been observed for modulation frequencies on the order comparable to photon count rate R_s, where signals start to be undersampled. Comparisons of SNR for two modulation frequencies f_m = 12 Hz and f_m = 120 kHz along the dark resonance indicate correlation of the decrease with fluorescence intensity, however the theoretical simulation of modulated fluorescence shows that the undersampling itself should not limit the observable

modulation frequency detection bandwidth. Simulation results did not show any decrease of SNR, even for the order of magnitude higher modulation frequencies then what was observed with the same photon rate. Other possible effects, including leaking of the spectral modulation sidebands out of the resonance slope or the frequency response of the AOM were also investigated and do not explain the observable decrease of SNR. The bandwidth of spectral modulation sidebands is given by the Carson rule, as described earlier. The response of the AOM was measured up to modulation frequency f_m = 1 MHz, but we measured flat response. At this point we thus leave the attainable frequency bandwidth limit of the presented method for further investigation, including studies of possible excitation of first or higher order motional sidebands within the employed Raman excitation scheme might play a role.

The sensitivity of the fluorescence to frequency detuning can be further improved. First option is to increase the fluorescence detection efficiency, which has been in our case mostly limited by the numerical aperture of the collection optics to 0.15% of the total emission rate. The other option is to increase the number of trapped ions. Both options will linearly enhance fluorescence intensity and thus also the steepness of the dark resonance slope.

Chapter 9

Conclusion

In the first part of this thesis we have demonstrated that long distances can be measured with high accuracy using a mode-filtered frequency comb and a simple linear array spectrometer based on a diffraction grating. In comparison to a HeNe laser a relative agreement below 10^{-8} has been shown. The method of cavity mode filtering opens up the possibility to use a low repetition rate frequency comb, like a fiber comb, for many-wavelength homodyne interferometry. Since fiber combs are smaller, easier to operate and less sensitive to the environment than Ti:Sapphire-based combs, this could be of interest for potential field applications of this method using fiber combs. When using a filter cavity to generate repetition rates of several 10s of GHz, it is possible to replace the complicated VIPA spectrometer with a linear array spectrometer. This not only simplifies the experimental setup, it also simplifies data processing and analysis.

The filter cavity constructed for the purpose of the distance measurements has been designed to work in a Vernier configuration, which allows for a large tuning of filter ratio with fractional change of cavity length. This also enables to obtain high repetition rates of 100s GHz with relatively large cavity lengths, which simplifies its construction. Even easier operation of a filter cavity has been investigated using all fiber approach. A fiber filter cavity has been designed and constructed to work with fiber frequency combs at 1550 nm. The performance of the silver coated fiber cavity to multiply f_{rep} from 0.1 to 1 Ghz was successfully tested using the VIPA spectrometer.

In general, the availability of frequency combs having a mode spacing that is sufficiently large to be resolved by an array spectrometer, will be a step forward towards practical applications of many-wavelength homodyne interferometry for absolute distance measurement.

In the second part of this thesis we have used a frequency comb as the optical reference for investigation of a method of optical frequency analysis using fluorescence emitted from a single Doppler cooled $^{40}Ca^{+}$ ion trapped in a Paul trap. The method is based on enhanced fluorescence sensitivity to optical frequency fluctuations due to the probing of the ion close to a dark state in a lambda-like three level system. The ion's dark resonance represents a convertor of the relative optical frequency difference to the intensity of fluorescence. The characterization of this method has been carried out by deterministic modulation of relative frequency detuning of the two excitation laser at 397 and 866 nm which has been phase locked to the frequency comb. In this way they adopt known frequency linewidths and stability of the optical reference.

For the analysis of the ion fluorescence response to the laser frequency modulation a simple theoretical model of fluorescence signal to noise ratio has been developed. Its comparison with signal to noise data obtained by the Fourier analysis of measured fluorescence showed good agreement, however also certain limits of this method. We have shown that for applied measurement settings, the fundamental upper limit for optical frequency bandwidth is 8 Mhz and the lowest detectable laser frequency deviation is 2 kHz. The comparison of the theory with the presented measurements have also shown a decrease of signal to noise ratio for modulation frequencies on magnitudes higher than photon count rate. The measurements also showed a correlation of the decrease with fluorescence intensity, however we have not proved that the signal undersampling is the cause. Other possible effects have been also investigated and do not explain the observable

decrease of signal to noise ratio, thus we had left the attainable frequency bandwidth limit of the presented method for further investigation.

The presented feasible bandwidths, which are in good agreement with theoretical model, can be further improved by increasing the fluorescence detection efficiency or by increasing the number of trapped ions, what would also led to improved sensitivity of the fluorescence to frequency deviations.

References

[1] T Udem, R Holzwarth, and TW Hansch. "Optical frequency metrology". In: *NATURE* 416.6877 (2002), 233–237. ISSN: 0028-0836. DOI: 10.1038/416233a.

[2] J Reichert et al. "Phase coherent vacuum-ultraviolet to radio frequency comparison with a mode-locked laser". In: *PHYSICAL REVIEW LETTERS* 84.15 (2000), 3232–3235. ISSN: 0031-9007. DOI: 10.1103/PhysRevLett.84.3232.

[3] SA Diddams et al. "Direct link between microwave and optical frequencies with a 300 THz femtosecond laser comb". In: *PHYSICAL REVIEW LETTERS* 84.22 (2000), 5102–5105. ISSN: 0031-9007. DOI: 10.1103/PhysRevLett.84.5102.

[4] H Schnatz et al. "First phase-coherent frequency measurement of visible radiation". In: *PHYSICAL REVIEW LETTERS* 76.1 (1996), 18–21. ISSN: 0031-9007. DOI: 10.1103/PhysRevLett.76.18.

[5] Seung-Woo Kim. "Combs rule". English. In: *NATURE PHOTONICS* 3.6 (2009), 313–314. ISSN: 1749-4885. DOI: 10.1038/nphoton.2009.86.

[6] R Holzwarth et al. "Optical frequency synthesizer for precision spectroscopy". In: *PHYSICAL REVIEW LETTERS* 85.11 (2000), 2264–2267. ISSN: 0031-9007. DOI: 10.1103/PhysRevLett.85.2264.

[7] M Hentschel et al. "Attosecond metrology". In: *NATURE* 414.6863 (2001), 509–513. ISSN: 0028-0836. DOI: 10.1038/35107000.

[8] A Baltuska et al. "Attosecond control of electronic processes by intense light fields". In: *NATURE* 421.6923 (2003), 611–615. ISSN: 0028-0836. DOI: 10.1038/nature01414.

[9] M. J. Thorpe and J. Ye. "Cavity-enhanced direct frequency comb spectroscopy". In: *APPLIED PHYSICS B-LASERS AND OPTICS* 91.3-4 (2008), 397–414. ISSN: 0946-2171. DOI: 10.1007/s00340-008-3019-1.

[10] Adam Lesundak et al. "THE FEMTOSECOND OPTICAL FREQUENCY COMB BASED TOOL FOR SPECTRAL ANALYSIS OF MOLECULAR ABSORBTION GASES". In: *NANOCON 2012, 4TH INTERNATIONAL CONFERENCE*. 4th International Conference on NANOCON, Brno, CZECH REPUBLIC, OCT 23-25, 2012. Tanger Ltd; Czech Soc New Mat & Technologies; Reg Ctr Adv Technologies & Mat; Mat Res Soc Serbia; Norsk Materialteknisk Selskap. 2012, 836–841. ISBN: 978-80-87294-35-2.

[11] T. Steinmetz et al. "Fabry-Perot filter cavities for wide-spaced frequency combs with large spectral bandwidth". In: *APPLIED PHYSICS B-LASERS AND OPTICS* 96.2-3 (2009), 251–256. ISSN: 0946-2171. DOI: 10.1007/s00340-009-3374-6.

[12] Christoph Gohle et al. "Frequency comb vernier spectroscopy for broadband, high-resolution, high-sensitivity absorption and dispersion spectra". In: *PHYSICAL REVIEW LETTERS* 99.26 (2007). ISSN: 0031-9007. DOI: 10.1103/PhysRevLett.99.263902.

[13] K Minoshima and H Matsumoto. "High-accuracy measurement of 240-m distance in an optical tunnel by use of a compact femtosecond laser". In: *APPLIED OPTICS* 39.30 (2000), 5512–5517. ISSN: 1559-128X. DOI: 10.1364/AO.39.005512.

[14] J Ye. "Absolute measurement of a long, arbitrary distance to less than an optical fringe". English. In: *OPTICS LETTERS* 29.10 (2004), 1153–1155. ISSN: 0146-9592. DOI: 10.1364/OL.29.001153.

[15] Parama Pal and Wayne H. Knox. "Self referenced Yb-fiber-laser frequency comb using a dispersion micromanaged tapered holey fiber". In: *OPTICS EXPRESS* 15.19 (2007), 12161–12166. ISSN: 1094-4087. DOI: 10.1364/OE.15.012161.

[16] BR Washburn et al. "Phase-locked, erbium-fiber-laser-based frequency comb in the near infrared". In: *OPTICS LETTERS* 29.3 (2004), 250–252. ISSN: 0146-9592. DOI: 10.1364/OL.29.000250.

[17] Yves Salvade et al. "High-accuracy absolute distance measurement using frequency comb referenced multiwavelength source". In: *APPLIED OPTICS* 47.14 (2008), 2715–2720. ISSN: 1559-128X. DOI: 10.1364/AO.47.002715.

[18] Sangwon Hyun et al. "Absolute length measurement with the frequency comb of a femtosecond laser". In: *MEASUREMENT SCIENCE AND TECHNOLOGY* 20.9 (2009). ISSN: 0957-0233. DOI: 10.1088/0957-0233/20/9/095302.

[19] M. Cui et al. "High-accuracy long-distance measurements in air with a frequency comb laser". In: *OPTICS LETTERS* 34.13 (2009), 1982–1984. ISSN: 0146-9592. DOI: 10.1364/OL.34.001982.

[20] Dong Wei et al. "Time-of-flight method using multiple pulse train interference as a time recorder". English. In: *OPTICS EXPRESS* 19.6 (2011), 4881–4889. ISSN: 1094-4087. DOI: 10.1364/OE.19.004881.

[21] Petr Balling et al. "Femtosecond frequency comb based distance measurement in air". In: *OPTICS EXPRESS* 17.11 (2009), 9300–9313. ISSN: 1094-4087. DOI: 10.1364/OE.17.009300.

[22] Joohyung Lee et al. "Time-of-flight measurement with femtosecond light pulses". In: *NATURE PHOTONICS* 4.10 (2010), 716–720. ISSN: 1749-4885. DOI: 10.1038/NPHOTON.2010.175.

[23] Ki-Nam Joo and Seung-Woo Kim. "Absolute distance measurement by dispersive interferometry using a femtosecond pulse laser". In: *OPTICS EXPRESS* 14.13 (2006), 5954–5960. ISSN: 1094-4087. DOI: 10.1364/OE.14.005954.

[24] S. A. van den Berg et al. "Many-Wavelength Interferometry with Thousands of Lasers for Absolute Distance Measurement". In: *PHYSICAL REVIEW LETTERS* 108.18 (2012). ISSN: 0031-9007. DOI: 10.1103/PhysRevLett.108.183901.

[25] I. Coddington et al. "Rapid and precise absolute distance measurements at long range". In: *NATURE PHOTONICS* 3.6 (2009), 351–356. ISSN: 1749-4885. DOI: 10.1038/NPHOTON.2009.94.

[26] Joohyung Lee et al. "Absolute distance measurement by dual-comb interferometry with adjustable synthetic wavelength". In: *MEASUREMENT SCIENCE AND TECHNOLOGY* 24.4 (2013). ISSN: 0957-0233. DOI: 10.1088/0957-0233/24/4/045201.

[27] Steven A. van den Berg, Sjoerd van Eldik, and Nandini Bhattacharya. "Mode-resolved frequency comb interferometry for high-accuracy long distance measurement". English. In: *SCIENTIFIC REPORTS* 5 (2015). ISSN: 2045-2322. DOI: 10.1038/srep14661.

[28] M. T. Murphy et al. "High-precision wavelength calibration of astronomical spectrographs with laser frequency combs". In: *MONTHLY NOTICES OF THE ROYAL ASTRONOMICAL SOCIETY* 380.2 (2007), 839–847. ISSN: 0035-8711. DOI: 10.1111/j.1365-2966.2007.12147.x.

[29] Chih-Hao Li et al. "A laser frequency comb that enables radial velocity measurements with a precision of 1 cm s(-1)". In: *NATURE* 452.7187 (2008), 610–612. ISSN: 0028-0836. DOI: 10.1038/nature06854.

[30] D. A. Braje et al. "Astronomical spectrograph calibration with broad-spectrum frequency combs". In: *EUROPEAN PHYSICAL JOURNAL D* 48.1 (2008), 57–66. ISSN: 1434-6060. DOI: 10.1140/epjd/e2008-00099-9.

[31] Tilo Steinmetz et al. "Laser frequency combs for astronomical observations". In: *SCIENCE* 321.5894 (2008), 1335–1337. ISSN: 0036-8075. DOI: 10.1126/science.1161030.

[32] S. A. Diddams et al. "Improved signal-to-noise ratio of 10 GHz microwave signals generated with a mode-filtered femtosecond laser frequency comb". In: *OPTICS EXPRESS* 17.5 (2009), 3331–3340. ISSN: 1094-4087. DOI: 10.1364/OE.17.003331.

[33] G ALZETTA et al. "EXPERIMENTAL-METHOD FOR OBSERVATION OF RF TRANSITIONS AND LASER BEAT RESONANCES IN ORIENTED NA VAPOR". In: *NUOVO CIMENTO DELLA SOCIETA ITALIANA DI FISICA B-GENERAL PHYSICS RELATIVITY ASTRONOMY AND MATHEMATICAL PHYSICS AND METHODS* 36.1 (1976), 5–20. ISSN: 0369-3554. DOI: 10.1007/BF02749417.

[34] A ASPECT et al. "LASER COOLING BELOW THE ONE-PHOTON RECOIL ENERGY BY VELOCITY-SELECTIVE COHERENT POPULATION TRAPPING". English. In: *PHYSICAL REVIEW LETTERS* 61.7 (1988), 826–829. ISSN: 0031-9007. DOI: 10.1103/PhysRevLett.61.826.

[35] G Morigi, J Eschner, and CH Keitel. "Ground state laser cooling using electromagnetically induced transparency". In: *PHYSICAL REVIEW LETTERS* 85.21 (2000), 4458–4461. ISSN: 0031-9007. DOI: 10.1103/PhysRevLett.85.4458.

[36] D. T. C. Allcock et al. "Dark-resonance Doppler cooling and high fluorescence in trapped Ca-43 ions at intermediate magnetic field". In: *NEW JOURNAL OF PHYSICS* 18 (2016). ISSN: 1367-2630. DOI: 10.1088/1367-2630/18/2/023043.

[37] CF Roos et al. "Experimental demonstration of ground state laser cooling with electromagnetically induced transparency". In: *PHYSICAL REVIEW LETTERS* 85.26, 1 (2000), 5547–5550. ISSN: 0031-9007. DOI: 10.1103/PhysRevLett.85.5547.

[38] C Lisowski et al. "Dark resonances as a probe for the motional state of a single ion". In: *APPLIED PHYSICS B-LASERS AND OPTICS* 81.1 (2005), 5–12. ISSN: 0946-2171. DOI: 10.1007/s00340-005-1867-5.

[39] J. Rossnagel et al. "Fast thermometry for trapped ions using dark resonances". In: *NEW JOURNAL OF PHYSICS* 17 (2015). ISSN: 1367-2630. DOI: 10.1088/1367-2630/17/4/045004.

[40] Thorsten Peters et al. "Thermometry of ultracold atoms by electromagnetically induced transparency". In: *PHYSICAL REVIEW A* 85.6 (2012). ISSN: 1050-2947. DOI: 10.1103/PhysRevA.85.063416.

[41] Adam Lesundak et al. "High-accuracy long distance measurements with a mode-filtered frequency comb". English. In: *OPTICS EXPRESS* 25.26 (2017), 32570–32580. ISSN: 1094-4087. DOI: 10.1364/OE.25.032570.

[42] Joohyung Lee, Seung-Woo Kim, and Young-Jin Kim. "Repetition rate multiplication of femtosecond light pulses using a phase-locked all-pass fiber resonator". In: *OPTICS EXPRESS* 23.8 (2015), 10117–10125. ISSN: 1094-4087. DOI: 10.1364/OE.23.010117.

[43] Miguel A. Preciado and Miguel A. Muriel. "Repetition-rate multiplication using a single all-pass optical cavity". English. In: *OPTICS LETTERS* 33.9 (2008), 962–964. ISSN: 0146-9592. DOI: 10.1364/OL.33.000962.

[44] A. Haboucha et al. "Optical-fiber pulse rate multiplier for ultralow phase-noise signal generation". English. In: *OPTICS LETTERS* 36.18 (2011), 3654–3656. ISSN: 0146-9592. DOI: 10.1364/OL.36.003654.

[45] Yoshiaki Nakajima, Akiko Nishiyama, and Kaoru Minoshima. "Mode-filtering technique based on all-fiber-based external cavity for fiber-based optical frequency comb". In: *OPTICS EXPRESS* 26.4 (2018), 4656–4664. ISSN: 1094-4087. DOI: 10.1364/OE.26.004656.

[46] ST Cundiff, J Ye, and JL Hall. "Optical frequency synthesis based on mode-locked lasers". English. In: *REVIEW OF SCIENTIFIC INSTRUMENTS* 72.10 (2001), 3749–3771. ISSN: 0034-6748. DOI: 10.1063/1.1400144.

[47] Adam Lesundak et al. "Single trapped ion fluorescence response to frequency modualtion of dark state popupation". to be submitted. 2019.

[48] JR Carson. "Notes on the theory of modulation". English. In: *PROCEEDINGS OF THE INSTITUTE OF RADIO ENGINEERS* 10.1 (1922), 57–64. ISSN: 0731-5996. DOI: 10.1109/JRPROC.1922.219793.

[49] RJ Pieper. "Laboratory and computer tests for Carson's FM bandwidth rule". In: *PROCEEDINGS OF THE 33RD SOUTHEASTERN SYMPOSIUM ON SYSTEM THEORY*. PROCEEDINGS - SOUTHEASTERN SYMPOSIUM ON SYSTEM THEORY. 33rd Southeastern Symposium on System Theory, OHIO UNIV, ATHENS, OH, MAR 18-20, 2001. Russ Coll Engn & Technol; Sch Elect Engn & Comp Sci; IEEE Control Soc; IEEE. 2001, 145–149. ISBN: 0-7803-6661-1. DOI: 10.1109/SSST.2001.918507.

List of publications

[1] Adam Lesundak et al. “High-accuracy long distance measurements with a mode-filtered frequency comb”. English. In: *OPTICS EXPRESS* 25.26 (2017), 32570–32580. ISSN: 1094-4087. DOI: 10.1364/OE.25.032570.

[2] Adam Lesundak et al. “THE FEMTOSECOND OPTICAL FREQUENCY COMB BASED TOOL FOR SPECTRAL ANALYSIS OF MOLECULAR ABSORBTION GASES”. In: *NANOCON 2012, 4TH INTERNATIONAL CONFERENCE*. 4th International Conference on NANOCON, Brno, CZECH REPUBLIC, OCT 23-25, 2012. Tanger Ltd; Czech Soc New Mat & Technologies; Reg Ctr Adv Technologies & Mat; Mat Res Soc Serbia; Norsk Materialteknisk Selskap. 2012, 836–841. ISBN: 978-80-87294-35-2.

[3] Adam Lesundak et al. “Repetition rate multiplication of a femtosecond frequency comb”. In: *PHOTONICS, DEVICES, AND SYSTEMS VI*. Ed. by Tomanek, P and Senderakova, D and Pata, P. Vol. 9450. Proceedings of SPIE. 8th International Conference on Photonics, Devices, and System VI, Prague, CZECH REPUBLIC, AUG 27-29, 2014. Czech & Slovak Soc Photon; Act M Agcy. 2015. ISBN: 978-1-62841-566-7. DOI: 10.1117/12.2074415.

[4] Adam Lesundak et al. “Single trapped ion fluorescence response to frequency modualtion of dark state popupation”. to be submitted. 2019.

[5] Dirk Voigt et al. “High-accuracy absolute distance measurement with a mode-resolved optical frequency comb”. English. In: *OPTICAL SENSING AND DETECTION IV*. Ed. by Berghmans, F and Mignani, AG. Vol. 9899. Proceedings of SPIE. Conference on Optical Sensing and Detection IV, Brussels, BELGIUM, APR 03-07, 2016. SPIE; Brussels Photon Team; Res Fdn Flanders; Visit Brussels. 1000 20TH ST, PO BOX 10, BELLINGHAM, WA 98227-0010 USA: SPIE-INT SOC OPTICAL ENGINEERING, 2016. ISBN: 978-1-5106-0144-4. DOI: 10.1117/12.2227360.

[6] P. Obsil et al. “Nonclassical Light from Large Ensembles of Trapped Ions”. In: *PHYSICAL REVIEW LETTERS* 120.25 (2018). ISSN: 0031-9007. DOI: 10.1103/PhysRevLett.120.253602.

[7] L. Slodicka et al. “TRAPPING AND COOLING OF SINGLE IONS FOR FREQUENCY METROLOGY AND QUANTUM OPTICS EXPERIMENTS”. In: *RECENT TRENDS IN CHARGED PARTICLE OPTICS AND SURFACE PHYSICS INSTRUMENTATION*. Ed. by Mika, F. 15th International Seminar on Recent Trends in Charged Particle Optics and Surface Physics Instrumentation, Brno, CZECH REPUBLIC, MAY 29-JUN 03, 2016. Czech Acad Sci, Inst Sci Instruments. 2016, 68–69. ISBN: 978-80-87441-17-6.

[8] V. Hucl et al. “Automatic unit for measuring refractive index of air based on Ciddor equation and its verification using direct interferometric measurement method”. In: *OPTICAL MEASUREMENT SYSTEMS FOR INDUSTRIAL INSPECTION VIII*. Ed. by Lehmann, PH and Osten, W and Albertazzi, A. Vol. 8788. Proceedings of SPIE. Conference on Optical Measurement Systems

for Industrial Inspection VIII, Munich, GERMANY, MAY 13-16, 2013. SPIE. 2013. ISBN: 978-0-8194-9604-1. DOI: 10.1117/12.2020756.

[9] Lenka Pravdova et al. "Length characterization of a piezoelectric actuator travel with a mode-locked femtosecond laser". In: *OPTICAL MEASUREMENT SYSTEMS FOR INDUSTRIAL INSPECTION IX*. Ed. by Lehmann, P and Osten, W and Albertazzi, GA. Vol. 9525. Proceedings of SPIE. Conference on Optical Measurement Systems for Industrial Inspection IX, Munich, GERMANY, JUN 22-25, 2015. SPIE. 2015. ISBN: 978-1-62841-685-5. DOI: 10.1117/12.2190745.

[10] Tuan M. Pham et al. "ANALYSIS OF FREQUENCY NOISE PROPERTIES OF 729 NM EXTENDED CAVITY DIODE LASER WITH UNBALANCED MACH-ZEHNDER INTERFEROMETER". In: *20TH SLOVAK-CZECH-POLISH OPTICAL CONFERENCE ON WAVE AND QUANTUM ASPECTS OF CONTEMPORARY OPTICS*. Ed. by Mullerova, J and Senderakova, D and Ladanyi, L and Scholtz, L. Vol. 10142. Proceedings of SPIE. 20th Slovak-Czech-Polish Optical Conference on Wave and Quantum Aspects of Contemporary Optics (SCPOC), Jasna, SLOVAKIA, SEP 05-09, 2016. Univ Zilina, Fac Elect Engn, Inst Aurel Stadola; Univ Zilina, Fac Elect Engn, Dept Phys; Int Laser Ctr; Slovak Electrotechn Soc; Slovak Res & Dev Agcy; Czech & Slovak Soc Photon; Kvant s r o; OptiXs s r o. 2016. ISBN: 978-1-5106-0733-0; 978-1-5106-0734-7. DOI: 10.1117/12.2264455.

[11] Lenka Pravdova et al. "Length measurement in absolute scale via low-dispersion optical cavity". In: *20TH SLOVAK-CZECH-POLISH OPTICAL CONFERENCE ON WAVE AND QUANTUM ASPECTS OF CONTEMPORARY OPTICS*. Ed. by Mullerova, J and Senderakova, D and Ladanyi, L and Scholtz, L. Vol. 10142. Proceedings of SPIE. 20th Slovak-Czech-Polish Optical Conference on Wave and Quantum Aspects of Contemporary Optics (SCPOC), Jasna, SLOVAKIA, SEP 05-09, 2016. Univ Zilina, Fac Elect Engn, Inst Aurel Stadola; Univ Zilina, Fac Elect Engn, Dept Phys; Int Laser Ctr; Slovak Electrotechn Soc; Slovak Res & Dev Agcy; Czech & Slovak Soc Photon; Kvant s r o; OptiXs s r o. 2016. ISBN: 978-1-5106-0733-0; 978-1-5106-0734-7. DOI: 10.1117/12.2264452.

[12] Ondrej Cip et al. "Laser-induced fluorescence spectroscopy in tissue local necrosis detection". In: *OPTICAL INTERACTIONS WITH TISSUE AND CELLS XXV; AND TERAHERTZ FOR BIOMEDICAL APPLICATIONS*. Ed. by Jansen, ED and Thomas, RJ and Wilmink, GJ and Ibey, BL. Vol. 8941. Proceedings of SPIE. Conference on Optical Interactions with Tissue and Cells XXV and Terahertz for Biomedical Applications, San Francisco, CA, FEB 02-04, 2014. SPIE. 2014. ISBN: 978-0-8194-9854-0. DOI: 10.1117/12.2052637.

[13] Tomas Pikalek et al. "Phase and group refractive indices of air calculation by fitting of phase difference measured using a combination of laser and low-coherence interferometry". In: *OPTICAL MEASUREMENT SYSTEMS FOR INDUSTRIAL INSPECTION X*. Ed. by Lehmann, P and Osten, W and Goncalves, AA. Vol. 10329. Proceedings of SPIE. Conference on Optical Measurement Systems for Industrial Inspection X part of the SPIE Optical Metrology Symposium, Munich, GERMANY, JUN 26-29, 2017. SPIE. 2017. ISBN: 978-1-5106-1104-7; 978-1-5106-1103-0. DOI: 10.1117/12.2269952.

[14] Peter Obšil et al. *Hydrogen pressure at 1012 mBar level in a room temperature ion trapping apparatus*. URL: https://arxiv.org/abs/1904.13242.

[15] Peter Obšil et al. *Scalable interference from trapped ion chains*. URL: https://arxiv.org/abs/1804.01518.

Souhrn v českém jazyce

Tato disertační práce se zabývá aplikací optického frekvenčního hřebene ve dvou odvětvích základní metrologie: měření vzdáleností a měření optických frekvencí. První část práce prezentuje homodynní interferometrii s módově filtrovaným frekvenčním hřebenem efektní metodu pro měření dlouhých vzdáleností si vysokou přesností a absolutní škálou. Princip měření vyžaduje, aby jednotlivé módy frekvenčního hřebene byli spektrálně rozlišitelné. Z tohoto důvodu nelze tuto metodu použít přímo s frekvenčními hřebeny s nízkou opakovací frekvencí (např. 100 MHz), protože jednotlivé módy jsou příliš blízko u sebe a nelze je rozlišit. Na zvýšení opakovací frekvence je zde využito filtrování módu pomocí optického rezonátoru a takto filtrovaný frekvenční hřeben je pak použit k měření absolutních vzdáleností. Módová filtrace je realizována pomocí Fabry-Pérotovho rezonátoru ve Vernierovské konfiguraci, co umožňuje dosažení opakovacích frekvencí v rozsahu od desítek GHz do více jak 100 GHz. Je demonstrováno, že vysoké módové rozestupy významně redukují požadavky na rozlišení spektrometru a umožňují absolutní měření vzdálenosti s módove filtrovaným hřebenem s použitím jednoduchého řádkového spektrometru pro detekci. Použit je 1 GHz hřeben, který je filtračním rezonátorem konvertován na 56 GHz. Je ukázáno, že porovnání s konvenčním relativním interferometrem je dosažena shoda v měření vzdáleností až do 50 m na úrovni 0.5 mikrometru.

Druhá část dizertační práce prezentuje metodu využívající zachyceného iontu vápníku $^{40}Ca^{+}$ jako převodníku z optických frekvencí do intenzity fluorescence pro optickou frekvenční analýzu laserů interagujících s iontem. Metoda je založená na analýze fluorescence emitované z iontu v temném stavu, který je vybuzen dvěma lasery s modulovaným vzájemným frekvenčním odladěním. Odezva detekovaného fotonového toku na vzájemné frekvenční odchylky je měřena na svahu temné rezonance vytvořené v lambda energetické struktuře, která koresponduje s dvěma dipólovými optickými přechody. Oba využívané lasery jsou fázově zavěšeny na optický frekvenční hřeben, což umožňuje přesnou kalibraci metody deterministickým modulováním frekvence analyzovaného laseru vzhledem k fixní referenční frekvenci. Měřená fluorescenční odezva je vyhodnocována s použitím Fourierovy analýzy a výsledky jsou porovnány s teoretickým modelem pro dosažitelné poměry signálu k šumu pro škálu modulačních frekvencí a amplitud. Výsledky ukazují shodu s teorií pro určité rozsahy modulačních parametrů a taktéž vymezují limity metody ve smyslu detekovatelných frekvenčních odchylek a dosažitelných modulačních frekvencí.